30. Mullendore ME, Koorstra JB, Li YM, Offerhaus GJ, Fan X, et al. (2009) Ligand-dependent Notch signaling is involved in tumor initiation and tumor maintenance in pancreatic cancer. Clin Cancer Res 15: 2291–2301.
31. Stylianou S, Clarke RB, Brennan K (2006) Aberrant activation of notch signaling in human breast cancer. Cancer Res 66: 1517–1525.
32. Serafin V, Persano L, Moserle L, Esposito G, Ghisi M, et al. (2011) Notch3 signalling promotes tumour growth in colorectal cancer. J Pathol 224: 448–460.
33. Kuroda K, Tani S, Tamura K, Minoguchi S, Kurooka H, et al. (1999) Delta-induced Notch signaling mediated by RBP-J inhibits MyoD expression and myogenesis. J Biol Chem 274: 7238–7244.
34. Hirsinger E, Malapert P, Dubrulle J, Delfini MC, Duprez D, et al. (2001) Notch signalling acts in postmitotic avian myogenic cells to control MyoD activation. Development 128: 107–116.
35. Roma J, Masia A, Reventos J, Sanchez de Toledo J, Gallego S (2011) Notch pathway inhibition significantly reduces rhabdomyosarcoma invasiveness and mobility in vitro. Clin Cancer Res 17: 505–513.
36. Belyea BC, Naini S, Bentley RC, Linardic CM (2011) Inhibition of the Notch-Hey1 Axis Blocks Embryonal Rhabdomyosarcoma Tumorigenesis. Clin Cancer Res 17: 7324–7336.
37. Siemers ER, Quinn JF, Kaye J, Farlow MR, Porsteinsson A, et al. (2006) Effects of a gamma-secretase inhibitor in a randomized study of patients with Alzheimer disease. Neurology 66: 602–604.
38. van Es JH, van Gijn ME, Riccio O, van den Born M, Vooijs M, et al. (2005) Notch/gamma-secretase inhibition turns proliferative cells in intestinal crypts and adenomas into goblet cells. Nature 435: 959–963.
39. Tohda S, Sato T, Kogoshi H, Fu L, Sakano S, et al. (2006) Establishment of a novel B-cell lymphoma cell line with suppressed growth by gamma-secretase inhibitors. Leuk Res 30: 1385–1390.
40. Beel AJ, Sanders CR (2008) Substrate specificity of gamma-secretase and other intramembrane proteases. Cell Mol Life Sci 65: 1311–1334.
41. Zavadil J, Cermak L, Soto-Nieves N, Bottinger EP (2004) Integration of TGF-beta/Smad and Jagged1/Notch signalling in epithelial-to-mesenchymal transition. Embo J 23: 1155–1165.
42. Sarmento LM, Huang H, Limon A, Gordon W, Fernandes J, et al. (2005) Notch1 modulates timing of G1-S progression by inducing SKP2 transcription and p27 Kip1 degradation. J Exp Med 202: 157–168.
43. Abbas T, Dutta A (2009) p21 in cancer: intricate networks and multiple activities. Nat Rev Cancer 9: 400–414.
44. Pannuti A, Foreman K, Rizzo P, Osipo C, Golde T, et al. (2010) Targeting Notch to target cancer stem cells. Clin Cancer Res 16: 3141–3152.
45. Sullivan JP, Spinola M, Dodge M, Raso MG, Behrens C, et al. (2010) Aldehyde dehydrogenase activity selects for lung adenocarcinoma stem cells dependent on notch signaling. Cancer Res 70: 9937–9948.
46. Hirotsu M, Setoguchi T, Matsunoshita Y, Sasaki H, Nagao H, et al. (2009) Tumour formation by single fibroblast growth factor receptor 3-positive rhabdomyosarcoma-initiating cells. Br J Cancer 101: 2030–2037.
47. Sana J, Zambo I, Skoda J, Neradil J, Chlapek P, et al. (2011) CD133 expression and identification of CD133/nestin positive cells in rhabdomyosarcomas and rhabdomyosarcoma cell lines. Anal Cell Pathol 34: 1–16.
48. Walter D, Satheesha S, Albrecht P, Bornhauser BC, D'Alessandro V, et al. (2011) CD133 positive embryonal rhabdomyosarcoma stem-like cell population is enriched in rhabdospheres. PLoS One 6: e19506.
49. Schreck KC, Taylor P, Marchionni L, Gopalakrishnan V, Bar EE, et al. (2010) The Notch target Hes1 directly modulates Gli1 expression and Hedgehog signaling: a potential mechanism of therapeutic resistance. Clin Cancer Res 16: 6060–6070.

OPEN ACCESS Freely available online

PLOS | ONE

Dynamic Increase in Extracellular ATP Accelerates Photoreceptor Cell Apoptosis via Ligation of P2RX7 in Subretinal Hemorrhage

Shoji Notomi[1], Toshio Hisatomi[1,2]*, Yusuke Murakami[1], Hiroto Terasaki[3], Shozo Sonoda[3], Ryo Asato[1,2], Atsunobu Takeda[1], Yasuhiro Ikeda[1], Hiroshi Enaida[1], Taiji Sakamoto[3], Tatsuro Ishibashi[1]

1 Department of Ophthalmology, Graduate School of Medical Sciences, Kyushu University, Fukuoka, Japan, **2** Clinical Research Institute, National Hospital Organization Kyushu Medical Center, Fukuoka, Japan, **3** Department of Ophthalmology, Graduate School of Medical Sciences, Kagoshima University, Kagoshima, Japan

Abstract

Photoreceptor degeneration is the most critical cause of visual impairment in age-related macular degeneration (AMD). In neovascular form of AMD, severe photoreceptor loss develops with subretinal hemorrhage due to choroidal neovascularization (CNV), growth of abnormal blood vessels from choroidal circulation. However, the detailed mechanisms of this process remain elusive. Here we demonstrate that neovascular AMD with subretinal hemorrhage accompanies a significant increase in extracellular ATP, and that extracellular ATP initiates neurodegenerative processes through specific ligation of Purinergic receptor P2X, ligand-gated ion channel, 7 (P2RX7; P2X7 receptor). Increased extracellular ATP levels were found in the vitreous samples of AMD patients with subretinal hemorrhage compared to control vitreous samples. Extravascular blood induced a massive release of ATP and photoreceptor cell apoptosis in co-culture with primary retinal cells. Photoreceptor cell apoptosis accompanied mitochondrial apoptotic pathways, namely activation of caspase-9 and translocation of apoptosis-inducing factor (AIF) from mitochondria to nuclei, as well as TUNEL-detectable DNA fragmentation. These hallmarks of photoreceptor cell apoptosis were prevented by brilliant blue G (BBG), a selective P2RX7 antagonist, which is an approved adjuvant in ocular surgery. Finally, in a mouse model of subretinal hemorrhage, photoreceptor cells degenerated through BBG-inhibitable apoptosis, suggesting that ligation of P2RX7 by extracellular ATP may accelerate photoreceptor cell apoptosis in AMD with subretinal hemorrhage. Our results indicate a novel mechanism that could involve neuronal cell death not only in AMD but also in hemorrhagic disorders in the CNS and encourage the potential application of BBG as a neuroprotective therapy.

Citation: Notomi S, Hisatomi T, Murakami Y, Terasaki H, Sonoda S, et al. (2013) Dynamic Increase in Extracellular ATP Accelerates Photoreceptor Cell Apoptosis via Ligation of P2RX7 in Subretinal Hemorrhage. PLoS ONE 8(1): e53338. doi:10.1371/journal.pone.0053338

Editor: Mike O. Karl, Center for Regenerative Therapies Dresden, Germany

Received August 11, 2012; **Accepted** November 27, 2012; **Published** January 8, 2013

Copyright: © 2013 Notomi et al. This is an open-access article distributed under the terms of the Creative Commons Attribution License, which permits unrestricted use, distribution, and reproduction in any medium, provided the original author and source are credited.

Funding: This study was supported by a Grant-In-Aid for Scientific Research (number 21791690) from the Ministry of Education, Culture, Sports, Science, and Technology, Japan. The funders had no role in study design, data collection and analysis, decision to publish, or preparation of the manuscript.

Competing Interests: The authors have declared that no competing interests exist.

* E-mail: hisatomi@med.kyushu-u.ac.jp

Introduction

Age-related macular degeneration (AMD) is the leading cause of irreversible vision loss in the elderly in the developed world [1]. Among Americans, the estimated prevalence of AMD is projected to increase by more than 50% by the year 2020 [2]. In the neovascular form of this disorder, severe visual loss commonly occurs as a result of the invasion of abnormal blood vessels from the choroidal circulation, namely choroidal neovascularization (CNV), which induces irreversible damage to the overlying retina [3]. CNV could be induced by focally increased inflammatory and proangiogenic factors and/or by a decrease in anti-angiogenic factors. Various clinical as well as experimental studies have shown that vascular endothelial growth factor (VEGF), a proangiogenic glycoprotein, could be the most important factor for development of CNV [4]. In recent years, pharmacological inhibition of VEGF has offered the first opportunity to improve visual outcomes in patients diagnosed with this disorder [5]. Intraocular injections of an anti-VEGF antibody, such as ranibizumab or bevacizumab, have improved visual outcomes in several clinical trials [6]. However, patients with predominant subretinal hemorrhage, a commonly encountered event in neovascular AMD, still have poor visual prognoses [7]. Pneumatic displacement or surgical evacuation of subretinal blood with the use of recombinant tissue plasminogen activator (tPA) failed to improve the visual outcomes of patients with submacular hemorrhage due to AMD in a controlled clinical trial [8].

The most crucial stage of severe visual impairment is photoreceptor loss due to development of the CNV and related events such as subretinal hemorrhage or exudative retinal detachment in neovascular AMD [3]. Several clinical and experimental studies have shown that subretinal hemorrhage induces severe photoreceptor cell apoptosis [9–10] in line with severe tissue damage due to subarachnoid or intracerebral hematoma in the central nervous system (CNS) [11–12]. Previous studies have found that several potential neurotoxic agents were released from extravascular blood, such as hemoglobin [13], iron [10] [14–15], or glutamate [16], indicating that neurotoxic agents released from extravascular blood can be potential therapeutic targets.

Photoreceptor degeneration involves the activation of several signaling pathways of regulated cell death that can constitute potential therapeutic targets. Accordingly, attempts have been made to inhibit caspases, which play major roles in the apoptotic machinery [17–18], although pharmacological pan-caspase inhibitors largely failed to preserve the structures and functions of photoreceptors [19–20]. Caspases can be activated as a result of mitochondrial outer membrane permeabilization (MOMP) and the subsequent mitochondrial release of cytochrome *c* that triggers the Apaf-1 (apoptotic protease activating factor 1) apoptosome activation. MOMP also results in the mitochondrial release of apoptosis-inducing factor (AIF), which translocates to the nucleus and participates in the caspase-independent peripheral chromatin condensation and large-scale DNA fragmentation [21]. These findings suggest the existence of redundant cell death mechanisms downstream of MOMP [19] [22–23].

An alternative strategy to inhibit the mitochondrial apoptotic pathway is to intercept the initiating upstream proapoptotic signals. Recently, adenosine-5′-triphosphate (ATP) has been discovered as a major extracellular messenger that can contribute to lethal signaling [24]. Extracellular ATP can act on purinergic receptors, which are classified into two classes, the ionotropic, ligand-gated P2X receptors and the metabotropic, G protein-coupled P2Y receptors [25]. Among the seven subtypes of mammalian P2X receptors [26], the P2X7 receptor (P2RX7) differs from other P2X receptor subtypes by its long cytoplasmic, carboxy-terminal tail (240 amino acids) and mediates cellular signals that can trigger cell death [27–28]. P2RX7 is widely expressed in various organs, including those of immune system [29] and central nervous system [30]. In the retina, P2RX7 is expressed in Müller glia [31] as well as in both inner and outer retinal neurons, including retinal ganglion cells [32] and photoreceptor cells [33–34]. Furthermore, Fletcher and her group reported that P2RX7 has physiological functions as a neurotransmitter receptor in the retina [35], while photoreceptor cells have been shown to undergo apoptosis in response to an excess of extracellular ATP [36]. Recently, we have shown that photoreceptor cell apoptosis involves P2RX7 activation with caspase-8, -9 cleavage and mitochondrio-nuclear translocation of AIF. Moreover, photoreceptor cell apoptosis can be attenuated by Brilliant Blue G (BBG), a pharmacological P2RX7 antagonist that acts by blocking the interaction between extracellular ATP and P2RX7 [37]. Indeed, BBG administration can confer neuroprotective effects in several models of Alzheimer's, Parkinson's disease, and spinal cord injury [38–40] as well as in the retina [41–42]. BBG is also known as an adjuvant approved for intraoperative use in ocular surgery. In chromovitrectomy, vital dyes are introduced to improve the visualization of intraocular tissues for specific procedures, such as internal limiting membrane (ILM) peeling during vitrectomy [43–44].

Hence, we hypothesized that ATP acting on P2RX7 is involved in the pathogenesis of photoreceptor loss in subretinal hemorrhage. To examine the clinical relevance of this hypothesis, we compared extracellular ATP concentrations in human vitreous samples from patients with retinal diseases, including AMD. Our results showed that increased extracellular ATP substantially contributes to photoreceptor loss and that BBG provides substantial neuroprotective effects in cases of subretinal hemorrhage.

Materials and Methods

Ethics Statement

Procedures using human samples were conducted in accordance with the Declaration of Helsinki and approved by the Kyushu University Institutional Review Board for Clinical Research. We obtained written informed consent from all the participants. All procedures using mice were performed in strict accordance with the guidelines for Association for Research in Vision and Ophthalmology (ARVO) and Proper Conduct of Animal Experiments (Science Council of Japan). The experimental protocol was approved by the Animal Care and Use Committee of Kyushu University. All efforts were made to minimize the number of animals used and their suffering.

Animals

Adult (8 weeks of age) male C57BL6JJcl mice (CLEA, Tokyo, Japan) and isogenic P2rx7$^{-/-}$ mice, the latter kindly provided by Pfizer Inc. (Gorton, CT), were used in this study. Recently, the rd8 (retinal degeneration 8) mutation was reported to be widely inherited across strains supplied by common commercial vendors and ES cell lines [45–46]. We confirmed that P2rx7$^{-/-}$ mice do not carry the rd8 mutation by DNA sequencing (Supporting Information S1). All procedures using mice were performed in strict accordance with the guidelines for Association for Research in Vision and Ophthalmology (ARVO) and Proper Conduct of Animal Experiments (Science Council of Japan). The experimental protocol was approved by the Animal Care and Use Committee of Kyushu University. All efforts were made to minimize the number of animals used and their suffering.

Human Vitreous Samples

Procedures using human samples were conducted in accordance with the Declaration of Helsinki and approved by the Kyushu University Institutional Review Board for Clinical Research. We obtained written informed consent from all the participants. Vitreous samples (1.0–1.2 ml) were collected from patients who underwent pars plana vitrectomy at the Vitreoretinal Center in Kyushu University Hospital and Kagoshima University Hospital, for the treatment of macular hole (MH, $n = 10$), epiretinal membrane (ERM, $n = 10$), or age-related macular degeneration (AMD) with vitreous hemorrhage (VH) ($n = 15$). The clinical characteristics of the patients are summarized in Table 1 and Supporting Information S2.

ATP Measurements

The ATP levels of collected samples (100 µl each in 96-well microplates; BD Falcon, Franklin Lakes, NJ) were immediately determined by using luciferin-luciferase reaction buffer (ATP bioluminescence assay kit, FL-AA; Sigma-Aldrich, St. Louis, MO) and a Flex Station 3 Multi-Mode Microplate Reader (Molecular

Table 1. Clinical characteristics of patients with MH, ERM, and AMD with VH.

Characteristics	MH	ERM	AMD with VH	*P*
n	10	10	15	
Age (years)				
Mean (SD)	67.9 (6.8)	70.7 (6.4)	70.7 (10.4)	NS
Gender, *n*				
Male	4	2	9	
Female	6	8	6	NS

The patients underwent pars plana vitrectomy and the collected vitreous samples were subjected to ATP measurement by luciferase assay. There were no significant differences in age or sex ratio among the three groups.
doi:10.1371/journal.pone.0053338.t001

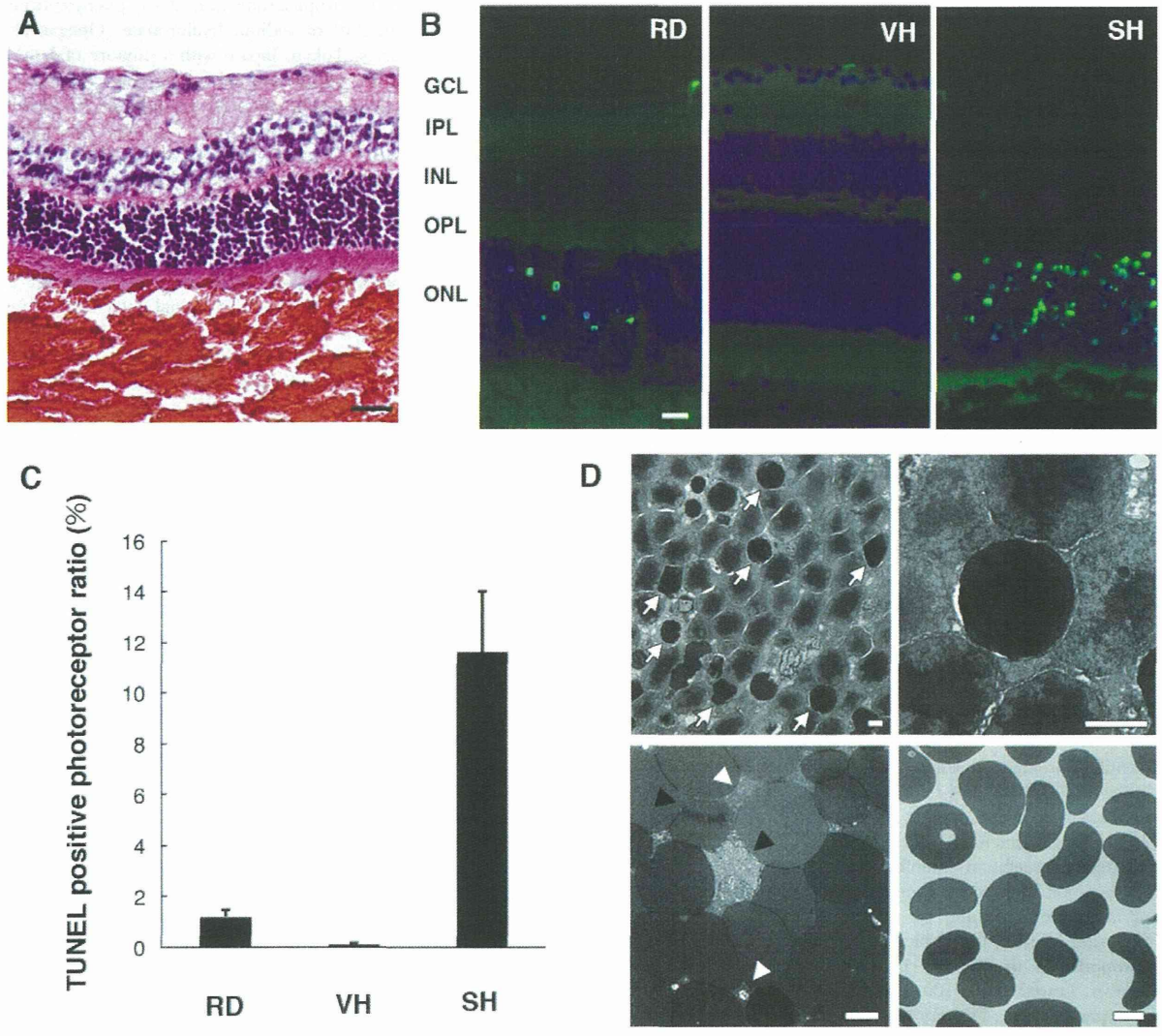

Figure 1. Abundant photoreceptor cell apoptosis in subretinal hemorrhage. Subretinal injection or vitreous injection of autologous blood was performed in C57BL6 mice. (A) A representative image of hematoxylin/eosin staining in subretinal hemorrhage is shown. Scale bar: 100 μm. (B) Some TUNEL$^+$ nuclei were detected in the outer nuclear layer (ONL) in retinal detachment (RD), while abundant TUNEL$^+$ nuclei were found in subretinal hemorrhage (SH). TUNEL$^+$ cells were less detectable in vitreous hemorrhage (VH) (TUNEL in green, propidium iodide in blue). Scale bar: 20 μm. GCL; ganglion cell layer, IPL; inner plexiform layer, INL; inner nuclear layer, OPL; outer plexiform layer, ONL; outer nuclear layer. (C) The numbers of TUNEL$^+$ photoreceptors in RD, VH, and SH. (D) Electron microscopy revealed that numerous photoreceptor cells had undergone apoptosis with chromatin condensation (arrows in the top left panel) or cellular shrinkage (top right panel). Some erythrocytes lost their plasma membranes (black arrowheads in the bottom left panel) and hemolytic debris was observed among erythrocytes (white arrowheads in the bottom left panel) in the subretinal hemorrhage. Minimal hemolytic change was observed in the vitreous hemorrhage (bottom right panel). Scale bars: 2 μm.
doi:10.1371/journal.pone.0053338.g001

Devices, Sunnyvale, CA). The ATP levels detected by the luminometer were expressed in relative light units (RLU).

Mouse Blood Collection

Mice were anesthetized with an intraperitoneal injection of pentobarbital and exsanguinated via cardiac puncture into collection tubes containing heparin. For the isolation of plasma, collected whole blood was immediately centrifuged at 18000 g for 60 seconds at 4°C to isolate plasma as previously described [47]. For the isolation of erythrocytes, the plasma, platelets, and leukocytes were removed as supernatant and buffy coat after centrifugation at 900 g for 3 min. Isolated erythrocytes were resuspended in medium supplemented with 0.5% bovine serum albumin to the corresponding final hematocrit. To determine ATP levels after hemolysis, whole blood or isolated erythrocytes were lysed in distilled water and then assayed using a firefly luciferase assay (FL-AA) as described above.

Adult Mouse Primary Retinal Cell Cultures

Adult primary retinal cell cultures were prepared as previously described with minor modifications [48] [22]. Primary retinal cells were cultured in 4-well chambers (Nunc; part of Thermo Fisher

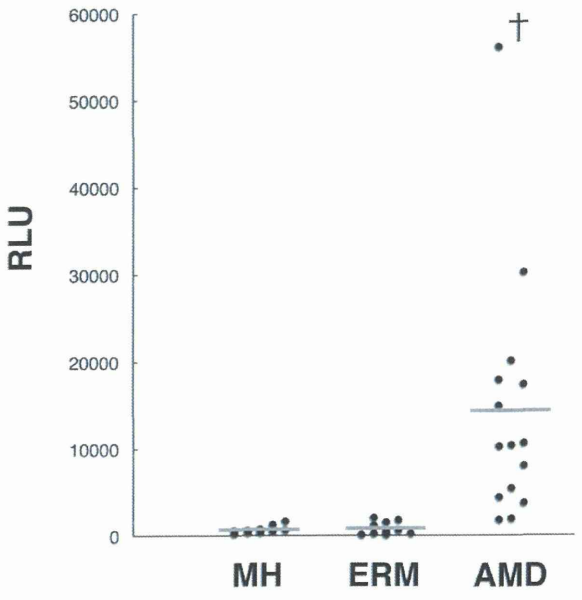

Figure 2. The ATP levels in human vitreous of retinal diseases. Human vitreous samples were collected during vitreoretinal surgery from patients with MH ($n = 10$), ERM ($n = 10$), and AMD ($n = 15$). The ATP levels of vitreous samples were determined by luciferin-luciferase assay (RLU: relative light units). †$P<0.01$.
doi:10.1371/journal.pone.0053338.g002

Scientific, Bremen, Germany) with Neurobasal-A medium (Invitrogen, Carlsbad, CA) containing B27 supplement without antioxidants (NBA/B27AO−; Invitrogen), 1 μg/ml insulin, and 12 μg/ml gentamicin. To determine the number of adherent photoreceptor cells, immunofluorescent staining was performed with a rabbit anti-recoverin antibody (Millipore, Bedford, MA). For blood clot exposure, we utilized a double chamber system [49]. After 50 μl of whole blood was placed on membranes with micropores in the upper chamber (Transwell; Corning Life Sciences, Lowell, MA), 100 μl of culture medium was added to the upper chamber. Primary retinal cell cultures were prepared in the lower chamber and incubated with or without 10 U/ml apyrase (Sigma-Aldrich, St. Louis, MO) for 24 h. The culture medium was collected and centrifuged, and the ATP levels of supernatants were analyzed by the luciferin-luciferase assay. For exogenous ATP administration, 1 mM ATP (Sigma-Aldrich) was added to the culture medium, and the medium were incubated for 24 h with or without 30 min pre-incubation of BBG.

Viability Assay in Primary Retinal Cell Cultures

To assess the viability of primary retinal cells, we used calcein AM (2 μM) or MitoTracker Orange CMTMRos (200 nM; M7510; Invitrogen), added for 30 min to primary retinal cell cultures. Then, cultured cells were fixed with 4% paraformaldehyde and recoverin-labeled calcein$^+$ or CMTMRos$^+$ photoreceptor cells were counted in 10 random fields by blinded observers using ImageJ software. Values are given as the means ± SDs of 10 replicate wells.

Subretinal Injections

Experimental retinal detachment was performed as previously described [19] [22] [48] [50]. Mice were anesthetized with an intraperitoneal injection of pentobarbital, and their pupils were dilated with topical 1% tropicamide and 2.5% phenylephrine hydrochloride. Then, 2 μl of sodium hyaluronate (Opegan-Hi; Santen Pharmaceuticals, Tokyo, Japan) with a mixture of 1 mM ATP or vehicle PBS, was gently injected into the subretinal space with a 30-gauge needle through the sclera posterior to the limbus to produce focally detached retina. The injection of sodium hyaluronate reproducibly generated similar retinal detachments. Successful retinal detachment was confirmed by ophthalmoscopy and generally involved one third of the retina as previously described [51]. To establish a mouse model of subretinal hemorrhage, autologous blood with a mixture of 50 μM BBG or vehicle PBS was immediately injected into the subretinal space as previously described [10]. The height of retinal detachments was measured at the top of the detached retina in cryosections (Supporting Information S3). Subretinal injections were only performed in the right eye of each animal, and 6 eyes were examined in each group. The mice were sacrificed 24 h after treatment. Their eyes were harvested, frozen at nitrogen liquid temperature, and cryosectioned for histochemical examinations.

TdT-dUTP Terminal Nick-end Labeling (TUNEL)

TUNEL analysis and quantification of TUNEL-positive cells were performed as previously described using the ApopTag Fluorescein In Situ Apoptosis Detection Kit (Millipore) [22]. Nuclei were counter-stained with propidium iodide or Hoechst 33342. The center of the detached retina was photographed, and the TUNEL-positive cells in the outer nuclear layer (ONL) were counted by two blinded observers. The ratios of photoreceptor cell apoptosis were expressed as the percentage of TUNEL-positive nuclei among the total number of nuclei in the section, and the results are presented as the means ± SDs.

Electron Microscopy

The posterior segments of enucleated mouse eyes were fixed in PBS containing 1% glutaraldehyde and 1% paraformaldehyde, postfixed in veronal acetate buffer osmium tetroxide (2%), dehydrated in ethanol and water, and embedded in Epon. Ultrathin sections were cut from blocks and mounted on copper grids. The specimens were observed with an H-7770 transmission electron microscope (Hitachi, Tokyo, Japan).

Immunofluorescence

Immunofluorescence was performed with slight modifications to a previous method [22]. Briefly, rabbit anti-AIF (R&D Systems, Minneapolis, MN), anti-mouse cleaved caspase-9 (Cell Signaling Technology, Beverly, MA), and anti-recoverin (Millipore) were used as primary antibodies and incubated at 4°C overnight. Goat anti-rabbit IgGs conjugated to Alexa Fluor 546 or 647 (Invitrogen) were used as secondary antibodies and incubated at room temperature for 1 h.

Statistical Analysis

Statistical differences between the two groups were analyzed by means of the Mann–Whitney U-test. Multiple group comparison was performed by ANOVA followed by Tukey–Kramer adjustments. The sex ratio in each group was analyzed by Fisher's exact test. Differences were considered significant at $P<0.05$ (*) and $P<0.01$ (**). All values were expressed as the means ± SDs.

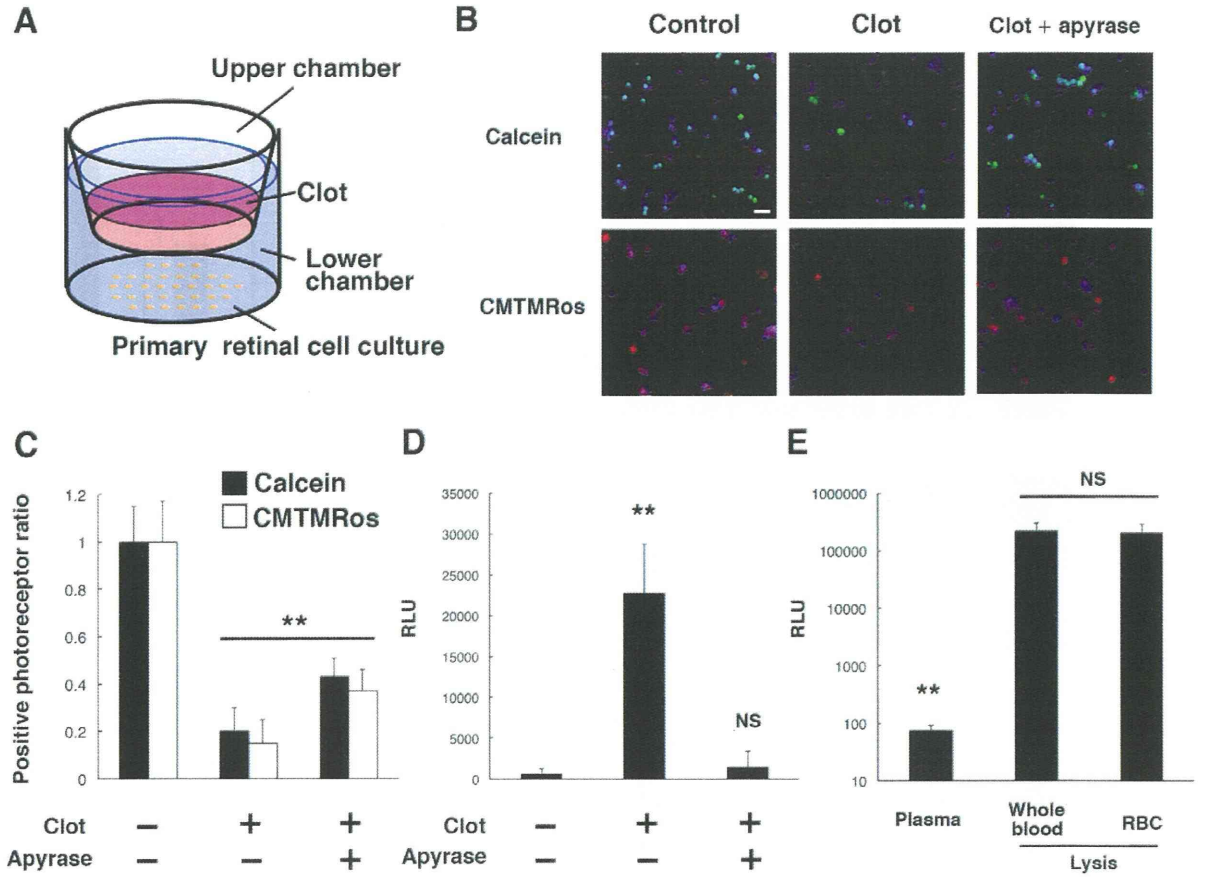

Figure 3. Photoreceptor cell apoptosis in primary retinal cell cultures with blood clots. (A) Schematic image of the double chamber co-culture system of primary retinal cells and blood clots. (B) and (C) The viability of primary retinal cells in the lower chamber was accessed by calcein AM or MitoTracker CMTMRos after 24 h of culture with addition of a clot in the upper chamber (calcein in green, CMTMRos in red, recoverin in blue). The frequency of calcein$^+$ or CMTMRos$^+$ photoreceptors significantly decreased after incubation with clots. Apyrase treatment significantly rescued photoreceptors. (D) The ATP levels of culture medium in the lower chamber were significantly increased by clot exposure, and reversed by apyrase treatment. (E) The ATP levels in plasma and blood. $n = 10$ per group; $^{**}P<0.01$. Scale bar: 20 μm.
doi:10.1371/journal.pone.0053338.g003

Results

Abundant Photoreceptor Cell Apoptosis in a Mouse Model of Subretinal Hemorrhage

To investigate the clinically relevant pathology of photoreceptor cell death in neovascular AMD, we created a mouse model of subretinal hemorrhage. Autologous blood drawn from the tail vein was injected into the subretinal space (Figure 1A). Retinal cell death has also been shown to occur after detachment of neurosensory retina [19] [52]. To evaluate the toxicity of subretinal blood to the overlying retina, a control condition was established by performing the retinal detachment using subretinal injections of sodium hyaluronate in line with our previous methods [19]. We examined the height of retinal detachment after injections of sodium hyaluronate or autologous blood and found no significant difference (Supporting Information S3). Abundant TUNEL$^+$ photoreceptor cells were detected in the outer nuclear layer (ONL) 24 h after the injections of autologous blood, while quite a small number of apoptotic photoreceptor cells were detected in control retinal detachment within 24 h (Figure 1, B and C). This result indicates that subretinal blood induces massive apoptotic photoreceptor cell death within 24 h and thus would cause irreversible visual impairment in the case of subretinal hemorrhage. Next, to investigate the toxicity of vitreous hemorrhage, autologous blood was injected into the vitreous cavity. Only a few TUNEL$^+$ cells were found after this injection in contrast to the case with subretinal hemorrhage (Figure 1, B and C), suggesting that a massive hemorrhage could severely reduce the integrity of photoreceptors, if it were tightly packed into the subretinal space. Moreover, electron microscopy revealed the characteristic signs of photoreceptor cell apoptosis, such as chromatin condensation or cellular shrinkage (Figure 1D). Numerous erythrocytes were observed in the subretinal clots. Some of those erythrocytes lost their plasma membranes with hemolytic debris 24 h after the injections, while minimal hemolytic change was observed in vitreous hemorrhage (Figure 1D). These observations suggest that potential neurotoxic factors were released from the blood clots during erythrocyte hemolysis.

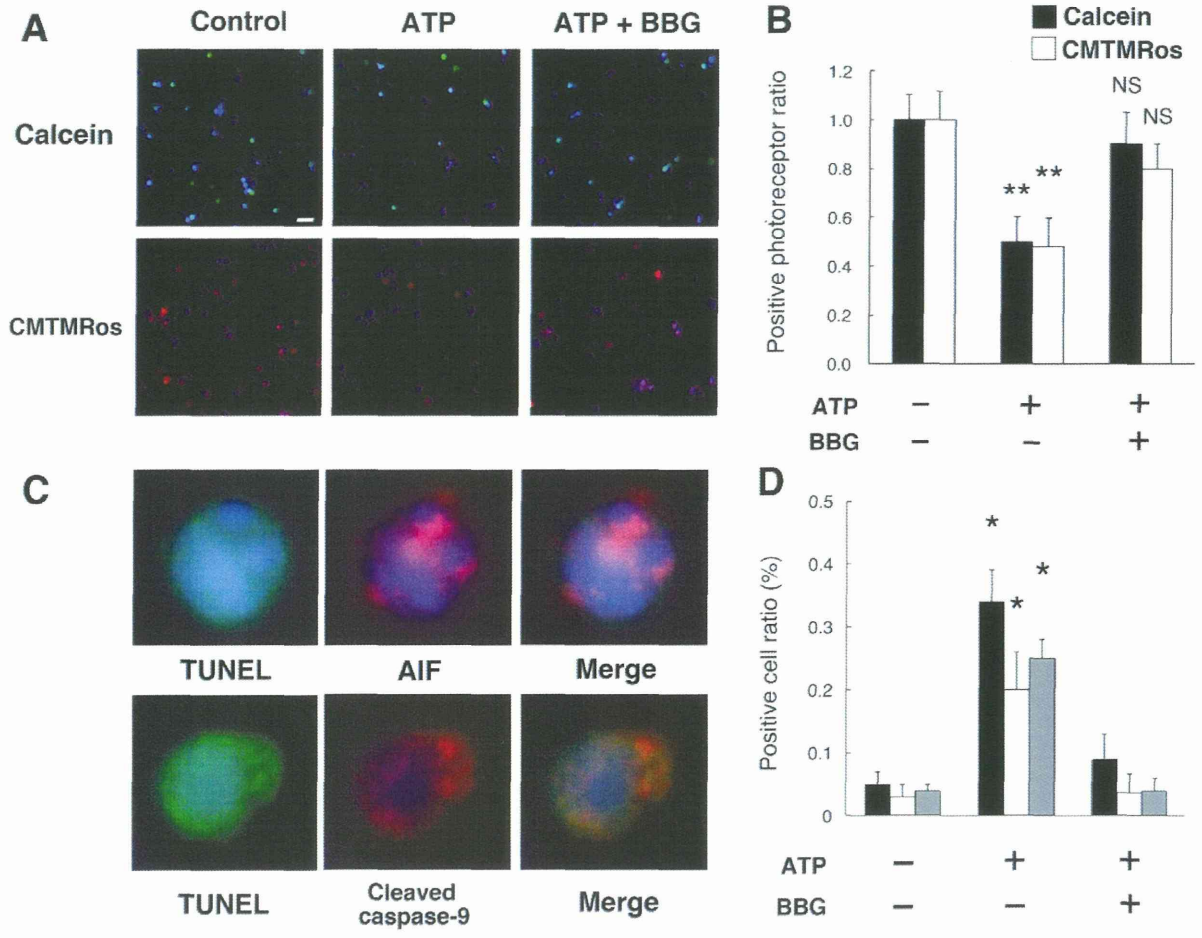

Figure 4. Photoreceptor cell apoptosis by ATP administration *in vitro*. (A) and (B) Calcein$^+$ or CMTMRos$^+$ photoreceptors were reduced by 24 h incubation of 1 mM ATP (calcein in green, CMTMRos in red, recoverin in blue). BBG notably attenuated the decline of viable photoreceptors. (C) and (D) Representative images of immuno-cytochemistry of AIF (top panels) and cleaved caspase-9 (bottom panels) in TUNEL$^+$ cells in primary retinal cell cultures (TUNEL in green, AIF or cleaved caspase-9 in red, Hoechst 33342 in blue) and the quantifications. $n = 10$ per group; $^*P<0.05$. $^{**}P<0.01$. Scale bar: 20 μm.
doi:10.1371/journal.pone.0053338.g004

Increased ATP Levels in the Vitreous of Patients with Age-related Macular Degeneration

To examine the potential role of extracellular ATP in subretinal hemorrhage, we investigated the intraocular concentrations of ATP by using vitreous samples collected during vitreoretinal surgery from patients with MH, ERM, or AMD with vitreous hemorrhage (VH). There is minimal breakdown of the blood retinal barrier (BRB)–i.e., exudation or bleeding–in MH or ERM. In contrast, vitreous hemorrhage–that is, diffusion of a large amount of blood into the vitreous cavity from the subretinal hemorrhage–often occurs in AMD, and in some of these cases vitrectomy is performed for removal of the vitreous opacity [53–54]. ATP levels of vitreous samples were analyzed by luciferin-luciferase assay, which is used to quantify chemiluminescence upon ATP-dependent oxidation of luciferin. Notably, ATP concentrations were much higher in AMD with VH compared to MH or ERM (Figure 2). These results suggest that ATP levels in the subretinal space could be potentially higher than those detected in the vitreous, because extracellular ATP diffuses into the vitreous cavity from the subretinal space. Hence, the local concentration of ATP around photoreceptors might be higher than the concentration of ATP observed in vitreous samples. Moreover, the increase in extracellular ATP may be neurotoxic to the overlying retina in subretinal hemorrhage.

Extracellular ATP Induces Neurotoxicity in Primary Retinal Cell Cultures with Blood Clot

To identify potential neurotoxic factors released from the extravascular blood clots, we prepared mouse primary retinal cells in double chamber slides. Primary mouse retinal cell cultures were prepared as previously described [22] [48] in the lower chamber, while mouse blood was added to the upper chamber on membranes with micropores (Figure 3A). In this double chamber system, released soluble factors can easily diffuse between two chambers, while the blood clot itself remains in the upper chamber. Primary retinal cell cultures were incubated for 24 h with or without addition of a clot to the upper chamber. The cultures were also examined in the absence or presence of 10 U/

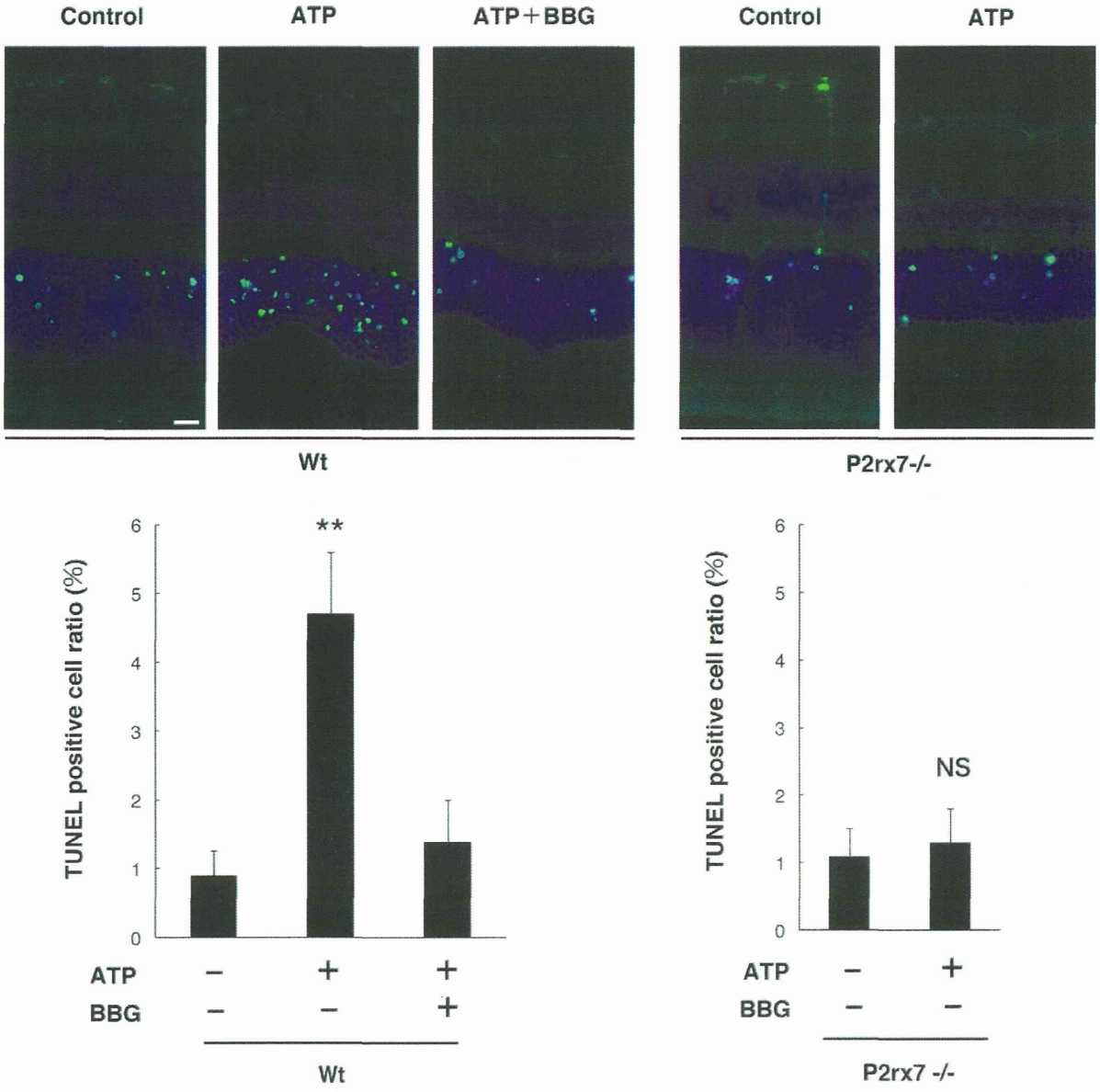

Figure 5. Photoreceptor cell apoptosis by subretinal injection of ATP. Exogenous ATP was injected into the subretinal space of Wt or P2rx7$^{-/-}$ mice. TUNEL-positive apoptotic cells developed in the ONL 24 h after the subretinal injection of 1 mM ATP (TUNEL in green and Hoechst 33342 in blue). $n=6$ per group; $^{**}P<0.01$. Scale bar: 20 μm.
doi:10.1371/journal.pone.0053338.g005

ml apyrase, a soluble ATP-degrading enzyme (ecto-ATPase) in the lower chamber. At 24 h of incubation, the clot showed a significant reduction in live photoreceptor cells (Figure 3, B and C), which were identified by two fluorescent live cell sensors, calcein AM and MitoTracker CMTMRos, which only label intact, non-apoptotic cells, and metabolically active cells, respectively. Of note, addition of apyrase, an ecto-ATPase, rescued photoreceptors from blood toxicity (Figure 3, B and C), suggesting that ATP released from clots was a critical factor in reducing photoreceptor cell survival. To confirm the ATP release from the clot, ATP levels in the lower chamber were analyzed by luciferase assay. The ATP levels were markedly elevated in the culture medium in the lower chamber after the addition of a clot in the upper chamber (Figure 3D). Apyrase treatment efficiently reversed the increase in ATP levels in the lower chamber (Figure 3D), demonstrating the contribution of extracellular ATP to the clot-induced toxicity consistent with the results of the cell viability assay. To clarify the source of extracellular ATP, we examined the ATP concentrations of mouse plasma. Only a small amount of ATP was detected in collected plasma, suggesting that the ATP levels in plasma were minimal under physiological conditions. However, massive ATP release was observed after hemolysis in whole blood (Figure 3E). In addition, ATP levels did not differ significantly between whole blood and isolated erythrocytes after hemolysis (Figure 3E),

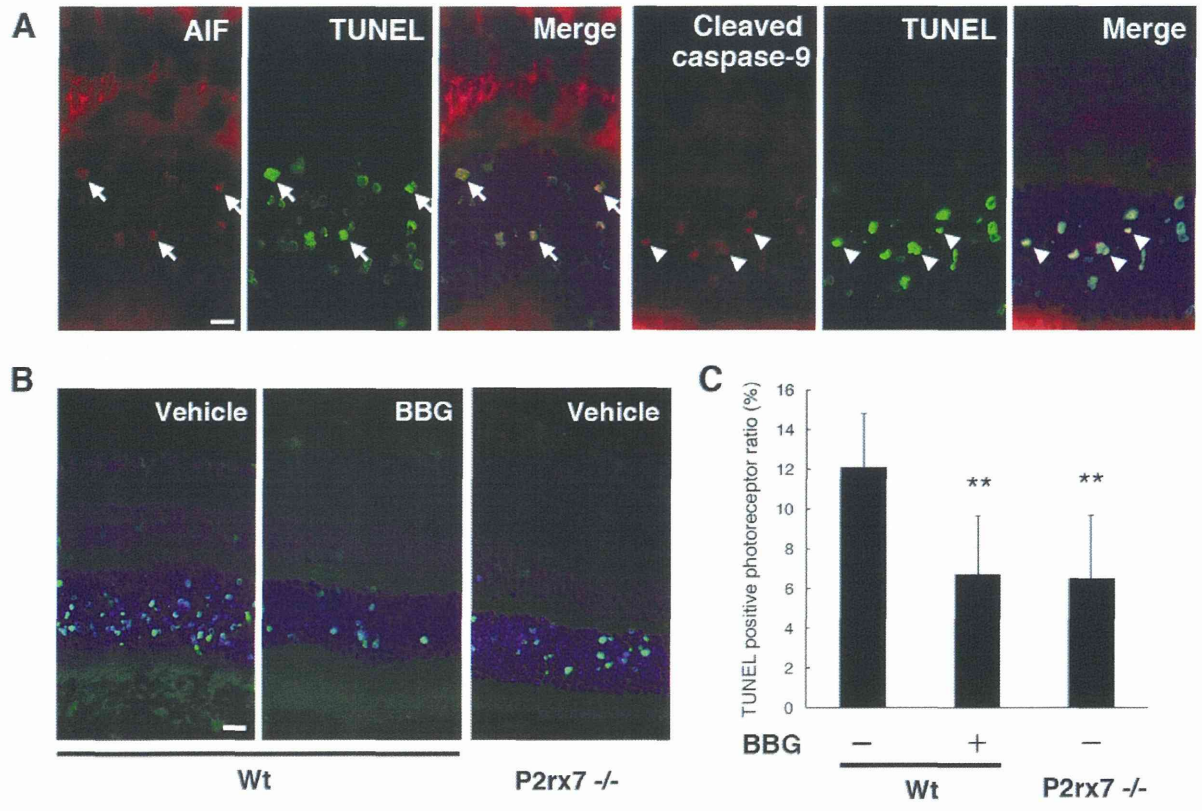

Figure 6. A P2RX7 antagonist prevents photoreceptor cell apoptosis in a mouse model of subretinal hemorrhage. (A) After the subretinal injection of autologous blood, photoreceptor cells underwent apoptotic cell death, and AIF-positive staining was observed in TUNEL$^+$ photoreceptor nuclei (arrows; AIF in red, TUNEL in green, and Hoechst 33342 in blue). Caspase-9 cleavage was also detected among TUNEL$^+$ nuclei (arrowheads; cleaved caspase-9 in red). Scale bar: 10 μm. (B) and (C) TUNEL$^+$ apoptotic cells in the absence or presence of 50 μM BBG treatment after experimental subretinal hemorrhage in Wt or P2rx7$^{-/-}$ mice. $n=6$ per group; $^{**}P<0.01$. Scale bar: 20 μm.
doi:10.1371/journal.pone.0053338.g006

indicating that erythrocytes could be a dominant source of extracellular ATP from clots. Taken together, these results suggest that released extracellular ATP may be a potential neurotoxic factor in neovascular AMD with subretinal hemorrhage.

Extracellular ATP Induces Photoreceptor Cell Apoptosis *in vitro* and *in vivo*

To obtain the mechanistic insights into the contribution of ATP/P2RX7 to photoreceptor death, we performed ATP administrations in primary culture. The addition of exogenous ATP significantly reduced viable, calcein$^+$ or CMTMRos$^+$ photoreceptor cells, while BBG reversed the decline in live photoreceptor cells (Figure 4, A and B). Furthermore, ATP administration induced TUNEL-detectable degradation of DNA with signs of the mitochondrial apoptotic pathway, namely AIF translocation to the nucleus and caspase-9 cleavage, whereas BBG treatment significantly inhibited those effects (Figure 4, C and D). These results indicate that extracellular ATP can trigger photoreceptor cell apoptosis via P2RX7-dependent machinery.

Next, we measured retinal cell apoptosis in the presence or absence of subretinal administration of exogenous ATP to determine whether the increase of subretinal ATP could trigger photoreceptor cell death *in vivo*. Exogenous ATP was mixed with sodium hyaluronate and injected into the subretinal space of C57BL/6 mice. We confirmed that the height of retinal detachment in the presence of the ATP mixture was not significantly different from that in the absence of ATP mixture (Supporting Information S3). Subretinal injections without ATP induced only limited TUNEL-positive apoptotic events in the ONL after 24 h of injections (Figure 5), whereas TUNEL-detectable DNA degradation was significantly accelerated by the administration of 1 mM ATP in the subretinal space (Figure 5). The increased photoreceptor cell apoptosis was substantially reduced by administration of 50 μM BBG (Figure 5). Furthermore, the numbers of TUNEL$^+$ photoreceptor cells were reduced in P2rx7$^{-/-}$ mice, while there was massive loss of photoreceptors in wild-type (Wt) mice (Figure 5), indicating that the induction of apoptosis by P2RX7 activation was truly specific. Thus, ATP administration substantially mimicked the effects of ATP release from clots. Taken together, these results showed that excessive ATP facilitates photoreceptor cell apoptosis via P2RX7 activation *in vitro* and *in vivo*, indicating a pathological contribution of extracellular ATP in subretinal hemorrhage.

BBG Protects Photoreceptors in a Mouse Model of Subretinal Hemorrhage

The results obtained from clinical samples and the *in vitro* and *in vivo* experiments led us to investigate whether the pharmacological P2RX7 antagonist would have a beneficial effect on retinal damage in a more pathological setting–namely, an animal model

of subretinal hemorrhage. Autologous blood was injected into the subretinal space alone or with a mixture of BBG (50 μM). Twenty-four hours after experimental subretinal hemorrhage, abundant $TUNEL^+$ photoreceptor cells were detected in the ONL with AIF translocation to the nucleus and caspase-9 cleavage (Figure 6A) in line with our previous reports that photoreceptor cells undergo apoptosis via the mitochondrial pathway as a result of MOMP [22]. These effects were notably attenuated by local injection of BBG (Figure 6, B and C). Moreover, TUNEL-detectable photoreceptor cell apoptosis was reduced in $P2rx7^{-/-}$ mice compared to Wt mice (Figure 6, B and C). Taken together, these results demonstrate that pharmacological inhibition of P2RX7 could results in neuroprotection of photoreceptors in cases of subretinal hemorrhage.

Discussion

In the present work, we have shown that severe human hemorrhagic pathologies, in particular AMD, are accompanied by a dynamic increase in extracellular ATP, which worsens photoreceptor degeneration. ATP was released from extravascular blood in primary retinal cell cultures *in vitro* and in a model of subretinal hemorrhage *in vivo*, and triggered severe photoreceptor cell apoptosis via P2RX7 ligation. We also provided mechanistic insights into exogenous ATP-induced photoreceptor cell apoptosis via mitochondrial apoptotic pathways–namely, the activation of caspase-9 and the mitochondrio-nuclear translocation of AIF. To our knowledge, this is the first report on pathogenic increase of extracellular ATP in hemorrhagic disorders in the retina as well as in the CNS. Finally, we demonstrated that BBG, a pharmacological P2RX7 antagonist, could correct photoreceptor cell death in a rodent model of subretinal hemorrhage.

The clinical application of anti-VEGF antibodies has enabled the regulation of CNV progression in patients with AMD worldwide [6]. However, patients still tend to have poor prognosis in neovascular AMD after massive subretinal hemorrhage. AMD as well as intracerebral hemorrhage causes severe tissue damage, suggesting that extravascular blood may become highly toxic to surrounding cells through the release of toxins [49]. In the current study, based on *in vitro* and *in vivo* models of blood neurotoxicity, we proposed a novel pathological pathway by which extracellular ATP could mediate mitochondrial apoptotic signaling. Moreover, we found that extracellular ATP levels can substantially increase in the presence of subretinal hemorrhage. Several potential mechanisms may account for the increase in extracellular ATP in hemophagic disorders. Acute cell lysis could be a source of ATP, in line with previous observations that ATP is released by acute stresses such as ischemia [55], hypotony [56], or oxygen/glucose deprivation [57]. In the present study, we observed that some erythrocytes underwent hemolysis under the retina and that blood clot exposure caused significant elevation of extracellular ATP *in vitro*. Hence, hemolysis could be a part of the cause of the ATP increase in subretinal hemorrhage. Moreover, the massive ATP release may be caused by usurpation of the physiological mechanism of release. Indeed, erythrocytes are sensitive to low oxygen supply and upregulate ATP efflux to modulate vascular tone via P2Y receptors on the endothelium [58]. These effluxes of ATP from erythrocytes may account for the findings that there were sustained elevation of ATP levels in the vitreous samples from AMD but not in those from MH or ERM.

Our results demonstrated that subretinal hemorrhage induced massive photoreceptor cell apoptosis, while the level of apoptosis was limited in cases of vitreous hemorrhage. The finding that vitreous hemorrhage induced minimal retinal cell apoptosis could be explained as follows. First, ATP concentrations around photoreceptors could be much higher in conditions in which blood clots are tightly packed in the subretinal space, while ATP can rapidly disperse into the vitreous space in cases of vitreous hemorrhage. In addition, subretinal injections of toxic agents have a greater risk of toxicity than vitreous injections [59–60]. The difference in the effect between intravitreous and subretinal injections was found to be more than 40-fold. This might be due to the presence of internal limiting membrane (ILM) and Müller glial cells that separate the vitreous cavity and neural retina, or the various cellular sensitivities to the specific stimulant. Another plausible explanation for the various sensitivities to extracellular ATP is localization of ecto-nucleoside triphosphate diphosphohydrolases (NTPDase) in the retina. NTPDase 1 and NTPDase 2 are mainly located in the ganglion cell layer (GCL), inner plexiform layer (IPL), and outer plexiform layer (OPL), indicating synaptic localization. In the OPL, NTPDases mainly localize in post-synaptic processes but not photoreceptor terminals [61]. In subretinal hemorrhage, ATP released from blood might be degraded by NTPDase during its diffusion through those synaptic layers, while photoreceptors could be exposed to ATP before its degradation. Hence, photoreceptors rather than ganglion cells and other inner retinal cells may tend to undergo apoptosis. Also in the case of vitreous hemorrhage, ATP might be degraded during diffusion through NTPDase-abundant inner retinal layers, which could account for why ATP had less toxic effect in vitreous hemorrhage than in subretinal hemorrhage.

Our present results also showed that subretinal injections of ATP markedly accelerated photoreceptor cell apoptosis, whereas other cells in the retina underwent limited TUNEL-detectable apoptosis. However, ganglion cells are reported to undergo cell death in response to the vitreous injection of BzATP [62]. A possible explanation for this discrepancy is that the local ATP concentration might not be sufficient to induce cell death in the inner retina. In our experiment, the highest concentration of ATP is assumed to be localized around photoreceptor cells. In addition, the retinal pigment epithelium (RPE) may have played roles in the observed photoreceptor degeneration. RPE cells also express P2RX7 [63] and may undergo cell death by subretinal hemorrhage. RPE degeneration could further worsen the photoreceptor degeneration, because RPE provides neurotrophic factors essential for photoreceptor survival. Further investigations will be needed to elucidate the role of RPE and extracellular ATP in retinal degeneration.

BBG, a selective P2RX7 antagonist, has been shown to be a potential therapeutic agent in a mouse model of spinal cord injury [40] [64]. Hence, BBG administration may have a neuroprotective effect in neurodegenerative diseases potentially linked to excessive extracellular ATP. In this context, it is worth noting that BBG is a clinically approved adjuvant for the surgical procedure of chromovitrectomy. We have introduced BBG as a safe staining dye for chromovitrectomy and an increasing number of reports support the safety and efficacy of BBG [44] [65–68]. Taken together, these findings demonstrate that BBG is biocompatible with ocular tissues, including neurosensory retina. Our results further encourage the potential application of BBG as a neuroprotective agent in degenerative disorders, especially in ATP-releasing subretinal hemorrhage. Furthermore, we have also reported that dying cells could release their own intracellular ATP into the extracellular space, resulting in a positive feed-forward loop that worsens the surrounding tissue damage [37]. Our current study further suggests that similar severe neurodegenerative pathologies, such as subarachnoid hemorrhage or intracerebral hemorrhage, could be linked to important elevations of extracellular ATP,

accelerating neuronal cell death and irreversible tissue damage. P2RX7 antagonists including BBG may have a neuroprotective therapeutic effect in retinal diseases as well as in CNS diseases with excessive extracellular ATP.

Supporting Information

Supporting Information S1 Genotyping of the rd8 mutation by DNA sequencing in P2rx7$^{-/-}$ mice. Recently, the rd8 mutation has been reported to be widely inherited across strains supplied by common commercial vendors and ES cell lines [45–46]. To confirm that P2rx7$^{-/-}$ mice do not carry the rd8 mutation, we performed genotyping of the Crb1^{rd8} allele carrying a single base pair deletion in exon 9 of the Crb1 gene. PCR amplification using flanking primers (5′-GCC CCT GTT TGC ATG GAG GAA ACT-3′ and 5′- GCC CCA TTT GCA CAC TGA TGA C-3′) and subsequent DNA sequencing demonstrated that the genotype of P2rx7$^{-/-}$ mice is the wild type allele ($n = 6$). Ocular fundus examination also confirmed that P2rx7$^{-/-}$ mice have no phenotype of retinal degeneration, namely drusen-like lesions, which are found in mice carrying the rd8 mutation [46].
(PDF)

Supporting Information S2 Characteristics and clinical data in patients with vitreous hemorrhage due to AMD. About 2,000 AMD patients are referred to our Vitreoretinal Center every year. Patients undergo ophthalmologic examinations, including visual acuity testing with standardized refraction using decimal charts and slit-lamp biomicroscopy. Decimal fractions of visual acuity were converted to the logarithm of the minimal angle of resolution (LogMAR) according to previous reports [69–70]. The mean preoperative visual acuity in AMD with VH was 0.008/2.10 (decimal/LogMAR), ranging from light perception to 0.03. At the preoperative examinations, the ocular fundi were almost invisible due to vitreous hemorrhage in AMD patients who underwent vitrectomy. After surgical removal of the vitreous opacity, the area of subretinal hemorrhage was confirmed by a postoperative review of the video records. A large area of subretinal hemorrhage ranging 4 to 30 disc diameters that involves the macula was observed in the fundus of those patients.
(TIF)

Supporting Information S3 The height of retinal detachment by injections of sodium hyaluronate, sodium hyaluronate with a mixture of ATP, and autologous blood. The height of retinal detachment was measured as the length between the photoreceptor outer segment and RPE in cryosections. The mean lengths in the three groups were not significantly different.
(TIF)

Acknowledgments

We thank Mari Imamura and Fumiyo Morikawa (Kyushu University) for technical assistance.

Author Contributions

Conceived and designed the experiments: SN TH HE TI. Performed the experiments: SN HT YM. Analyzed the data: SN AT YI. Contributed reagents/materials/analysis tools: HT SS RA TS. Wrote the paper: SN TH YI HE TI.

References

1. Ferris FL 3rd, Fine SL, Hyman L (1984) Age-related macular degeneration and blindness due to neovascular maculopathy. Arch Ophthalmol 102: 1640–1642.
2. Klein R, Rowland ML, Harris MI (1995) Racial/ethnic differences in age-related maculopathy. Third National Health and Nutrition Examination Survey. Ophthalmology 102: 371–381.
3. Grossniklaus HE, Green WR (2004) Choroidal neovascularization. Am J Ophthalmol 137: 496–503.
4. Ishibashi T, Hata Y, Yoshikawa H, Nakagawa K, Sueishi K, et al. (1997) Expression of vascular endothelial growth factor in experimental choroidal neovascularization. Graefes Arch Clin Exp Ophthalmol 235: 159–167.
5. Jager RD, Mieler WF, Miller JW (2008) Age-related macular degeneration. N Engl J Med 358: 2606–2617.
6. Rosenfeld PJ (2011) Bevacizumab versus ranibizumab for AMD. N Engl J Med 364: 1966–1967.
7. Steel DH, Sandhu SS (2011) Submacular haemorrhages associated with neovascular age-related macular degeneration. Br J Ophthalmol 95: 1051–1057.
8. Bressler NM, Bressler SB, Childs AL, Haller JA, Hawkins BS, et al. (2004) Surgery for hemorrhagic choroidal neovascular lesions of age-related macular degeneration: ophthalmic findings: SST report no. 13. Ophthalmology 111: 1993–2006.
9. Dunaief JL, Dentchev T, Ying GS, Milam AH (2002) The role of apoptosis in age-related macular degeneration. Arch Ophthalmol 120: 1435–1442.
10. Bhisitkul RB, Winn BJ, Lee OT, Wong J, Pereira Dde S, et al. (2008) Neuroprotective effect of intravitreal triamcinolone acetonide against photoreceptor apoptosis in a rabbit model of subretinal hemorrhage. Invest Ophthalmol Vis Sci 49: 4071–4077.
11. Sacco RL, Wolf PA, Bharucha NE, Meeks SL, Kannel WB, et al. (1984) Subarachnoid and intracerebral hemorrhage: natural history, prognosis, and precursive factors in the Framingham Study. Neurology 34: 847–854.
12. Hua Y, Keep RF, Hoff JT, Xi G (2007) Brain injury after intracerebral hemorrhage: the role of thrombin and iron. Stroke 38: 759–762.
13. Regan RF, Panter SS (1996) Hemoglobin potentiates excitotoxic injury in cortical cell culture. J Neurotrauma 13: 223–231.
14. Glatt H, Machemer R (1982) Experimental subretinal hemorrhage in rabbits. Am J Ophthalmol 94: 762–773.
15. Nakamura T, Keep RF, Hua Y, Schallert T, Hoff JT, et al. (2004) Deferoxamine-induced attenuation of brain edema and neurological deficits in a rat model of intracerebral hemorrhage. J Neurosurg 100: 672–678.
16. Qureshi AI, Ali Z, Suri MF, Shuaib A, Baker G, et al. (2003) Extracellular glutamate and other amino acids in experimental intracerebral hemorrhage: an in vivo microdialysis study. Crit Care Med 31: 1482–1489.
17. Ellis HM, Horvitz HR (1986) Genetic control of programmed cell death in the nematode C. elegans. Cell 44: 817–829.
18. Yuan J, Shaham S, Ledoux S, Ellis HM, Horvitz HR (1993) The C. elegans cell death gene ced-3 encodes a protein similar to mammalian interleukin-1 beta-converting enzyme. Cell 75: 641–652.
19. Hisatomi T, Sakamoto T, Murata T, Yamanaka I, Oshima Y, et al. (2001) Relocalization of apoptosis-inducing factor in photoreceptor apoptosis induced by retinal detachment in vivo. Am J Pathol 158: 1271–1278.
20. Green DR, Kroemer G (2005) Pharmacological manipulation of cell death: clinical applications in sight? J Clin Invest 115: 2610–2617.
21. Susin SA, Lorenzo HK, Zamzami N, Marzo I, Snow BE, et al. (1999) Molecular characterization of mitochondrial apoptosis-inducing factor. Nature 397: 441–446.
22. Hisatomi T, Nakazawa T, Noda K, Almulki L, Miyahara S, et al. (2008) HIV protease inhibitors provide neuroprotection through inhibition of mitochondrial apoptosis in mice. J Clin Invest 118: 2023–2038.
23. Murakami Y, Ikeda Y, Yonemitsu Y, Onimaru M, Nakagawa K, et al. (2008) Inhibition of nuclear translocation of apoptosis-inducing factor is an essential mechanism of the neuroprotective activity of pigment epithelium-derived factor in a rat model of retinal degeneration. Am J Pathol 173: 1326–1338.
24. Dubyak GR, el-Moatassim C (1993) Signal transduction via P2-purinergic receptors for extracellular ATP and other nucleotides. Am J Physiol 265: C577–606.
25. Abbracchio MP, Burnstock G (1994) Purinoceptors: are there families of P2X and P2Y purinoceptors? Pharmacol Ther 64: 445–475.
26. Ralevic V, Burnstock G (1998) Receptors for purines and pyrimidines. Pharmacol Rev 50: 413–492.
27. Surprenant A, Rassendren F, Kawashima E, North RA, Buell G (1996) The cytolytic P2Z receptor for extracellular ATP identified as a P2X receptor (P2X7). Science 272: 735–738.
28. Ferrari D, Los M, Bauer MK, Vandenabeele P, Wesselborg S, et al. (1999) P2Z purinoreceptor ligation induces activation of caspases with distinct roles in apoptotic and necrotic alterations of cell death. FEBS Lett 447: 71–75.
29. Chused TM, Apasov S, Sitkovsky M (1996) Murine T lymphocytes modulate activity of an ATP-activated P2Z-type purinoceptor during differentiation. J Immunol 157: 1371–1380.
30. Deuchars SA, Atkinson L, Brooke RE, Musa H, Milligan CJ, et al. (2001) Neuronal P2X7 receptors are targeted to presynaptic terminals in the central and peripheral nervous systems. J Neurosci 21: 7143–7152.
31. Pannicke T, Fischer W, Biedermann B, Schadlich H, Grosche J, et al. (2000) P2X7 receptors in Muller glial cells from the human retina. J Neurosci 20: 5965–5972.

32. Mitchell CH, Lu W, Hu H, Zhang X, Reigada D, et al. (2009) The P2X(7) receptor in retinal ganglion cells: A neuronal model of pressure-induced damage and protection by a shifting purinergic balance. Purinergic Signal 5: 241–249.
33. Puthussery T, Fletcher EL (2004) Synaptic localization of P2X7 receptors in the rat retina. J Comp Neurol 472: 13–23.
34. Puthussery T, Yee P, Vingrys AJ, Fletcher EL (2006) Evidence for the involvement of purinergic P2X receptors in outer retinal processing. Eur J Neurosci 24: 7–19.
35. Vessey KA, Fletcher EL (2012) Rod and cone pathway signalling is altered in the P2X7 receptor knock out mouse. PLoS One 7: e29990.
36. Puthussery T, Fletcher E (2009) Extracellular ATP induces retinal photoreceptor apoptosis through activation of purinoceptors in rodents. J Comp Neurol 513: 430–440.
37. Notomi S, Hisatomi T, Kanemaru T, Takeda A, Ikeda Y, et al. (2011) Critical involvement of extracellular ATP acting on P2RX7 purinergic receptors in photoreceptor cell death. Am J Pathol 179: 2798–2809.
38. McLarnon JG, Ryu JK, Walker DG, Choi HB (2006) Upregulated expression of purinergic P2X(7) receptor in Alzheimer disease and amyloid-beta peptide-treated microglia and in peptide-injected rat hippocampus. J Neuropathol Exp Neurol 65: 1090–1097.
39. Diaz-Hernandez M, Diez-Zaera M, Sanchez-Nogueiro J, Gomez-Villafuertes R, Canals JM, et al. (2009) Altered P2X7-receptor level and function in mouse models of Huntington's disease and therapeutic efficacy of antagonist administration. FASEB J 23: 1893–1906.
40. Peng W, Cotrina ML, Han X, Yu H, Bekar L, et al. (2009) Systemic administration of an antagonist of the ATP-sensitive receptor P2X7 improves recovery after spinal cord injury. Proc Natl Acad Sci U S A 106: 12489–12493.
41. Zhang X, Zhang M, Laties AM, Mitchell CH (2005) Stimulation of P2X7 receptors elevates Ca2+ and kills retinal ganglion cells. Invest Ophthalmol Vis Sci 46: 2183–2191.
42. Sugiyama T, Oku H, Shibata M, Fukuhara M, Yoshida H, et al. (2010) Involvement of P2X7 receptors in the hypoxia-induced death of rat retinal neurons. Invest Ophthalmol Vis Sci 51: 3236–3243.
43. Rodrigues EB, Meyer CH, Kroll P (2005) Chromovitrectomy: a new field in vitreoretinal surgery. Graefes Arch Clin Exp Ophthalmol 243: 291–293.
44. Enaida H, Hisatomi T, Hata Y, Ueno A, Goto Y, et al. (2006) Brilliant blue G selectively stains the internal limiting membrane/brilliant blue G-assisted membrane peeling. Retina 26: 631–636.
45. Mehalow AK, Kameya S, Smith RS, Hawes NL, Denegre JM, et al. (2003) CRB1 is essential for external limiting membrane integrity and photoreceptor morphogenesis in the mammalian retina. Hum Mol Genet 12: 2179–2189.
46. Mattapallil MJ, Wawrousek EF, Chan CC, Zhao H, Roychoudhury J, et al. (2012) The Rd8 mutation of the Crb1 gene is present in vendor lines of C57BL/6N mice and embryonic stem cells, and confounds ocular induced mutant phenotypes. Invest Ophthalmol Vis Sci 53: 2921–2927.
47. Wood RE, Wishart C, Walker PJ, Askew CD, Stewart IB (2009) Plasma ATP concentration and venous oxygen content in the forearm during dynamic handgrip exercise. BMC Physiol 9: 24.
48. Nakazawa T, Hisatomi T, Nakazawa C, Noda K, Maruyama K, et al. (2007) Monocyte chemoattractant protein 1 mediates retinal detachment-induced photoreceptor apoptosis. Proc Natl Acad Sci U S A 104: 2425–2430.
49. Jaremko KM, Chen-Roetling J, Chen L, Regan RF (2010) Accelerated hemolysis and neurotoxicity in neuron-glia-blood clot co-cultures. J Neurochem 114: 1063–1073.
50. Trichonas G, Murakami Y, Thanos A, Morizane Y, Kayama M, et al. (2010) Receptor interacting protein kinases mediate retinal detachment-induced photoreceptor necrosis and compensate for inhibition of apoptosis. Proc Natl Acad Sci U S A.
51. Yang L, Bula D, Arroyo JG, Chen DF (2004) Preventing retinal detachment-associated photoreceptor cell loss in Bax-deficient mice. Invest Ophthalmol Vis Sci 45: 648–654.
52. Zacks DN, Hanninen V, Pantcheva M, Ezra E, Grosskreutz C, et al. (2003) Caspase activation in an experimental model of retinal detachment. Invest Ophthalmol Vis Sci 44: 1262–1267.
53. Sakamoto T, Sheu SJ, Arimura N, Sameshima S, Shimura M, et al. (2010) Vitrectomy for exudative age-related macular degeneration with vitreous hemorrhage. Retina 30: 856–864.
54. Jung JH, Lee JK, Lee JE, Oum BS (2010) Results of vitrectomy for breakthrough vitreous hemorrhage associated with age-related macular degeneration and polypoidal choroidal vasculopathy. Retina 30: 865–873.
55. Melani A, Turchi D, Vannucchi MG, Cipriani S, Gianfriddo M, et al. (2005) ATP extracellular concentrations are increased in the rat striatum during in vivo ischemia. Neurochem Int 47: 442–448.
56. Oike M, Kimura C, Koyama T, Yoshikawa M, Ito Y (2000) Hypotonic stress-induced dual Ca(2+) responses in bovine aortic endothelial cells. Am J Physiol Heart Circ Physiol 279: H630–638.
57. Liu HT, Sabirov RZ, Okada Y (2008) Oxygen-glucose deprivation induces ATP release via maxi-anion channels in astrocytes. Purinergic Signal 4: 147–154.
58. Burnstock G (2008) Dual control of vascular tone and remodelling by ATP released from nerves and endothelial cells. Pharmacol Rep 60: 12–20.
59. Lee JE, Yoon TJ, Oum BS, Lee JS, Choi HY (2003) Toxicity of indocyanine green injected into the subretinal space: subretinal toxicity of indocyanine green. Retina 23: 675–681.
60. Ueno A, Hisatomi T, Enaida H, Kagimoto T, Mochizuki Y, et al. (2007) Biocompatibility of brilliant blue G in a rat model of subretinal injection. Retina 27: 499–504.
61. Ricatti MJ, Alfie LD, Lavoie EG, Sevigny J, Schwarzbaum PJ, et al. (2009) Immunocytochemical localization of NTPDase1 and 2 in the neural retina of mouse and zebrafish. Synapse 63: 291–307.
62. Hu H, Lu W, Zhang M, Zhang X, Argall AJ, et al. (2010) Stimulation of the P2X7 receptor kills rat retinal ganglion cells in vivo. Exp Eye Res 91: 425–432.
63. Yang D, Elner SG, Clark AJ, Hughes BA, Petty HR, et al. (2011) Activation of P2X receptors induces apoptosis in human retinal pigment epithelium. Invest Ophthalmol Vis Sci 52: 1522–1530.
64. Wang Q, Wang L, Feng YH, Li X, Zeng R, et al. (2004) P2X7 receptor-mediated apoptosis of human cervical epithelial cells. Am J Physiol Cell Physiol 287: C1349–1358.
65. Hisatomi T, Enaida H, Matsumoto H, Kagimoto T, Ueno A, et al. (2006) Staining ability and biocompatibility of brilliant blue G: preclinical study of brilliant blue G as an adjunct for capsular staining. Arch Ophthalmol 124: 514–519.
66. Enaida H, Hisatomi T, Goto Y, Hata Y, Ueno A, et al. (2006) Preclinical investigation of internal limiting membrane staining and peeling using intravitreal brilliant blue G. Retina 26: 623–630.
67. Farah ME, Maia M, Rodrigues EB (2009) Dyes in ocular surgery: principles for use in chromovitrectomy. Am J Ophthalmol 148: 332–340.
68. Rodrigues EB, Penha FM, de Paula Fiod Costa E, Maia M, Dib E, et al. (2010) Ability of new vital dyes to stain intraocular membranes and tissues in ocular surgery. Am J Ophthalmol 149: 265–277.
69. Holladay JT (1997) Proper method for calculating average visual acuity. J Refract Surg 13: 388–391.
70. Schulze-Bonsel K, Feltgen N, Burau H, Hansen L, Bach M (2006) Visual acuities "hand motion" and "counting fingers" can be quantified with the freiburg visual acuity test. Invest Ophthalmol Vis Sci 47: 1236–1240.

Clinical Study

Oncology

Oncology 2012;83:158–164
DOI: 10.1159/000341390

Received: May 9, 2012
Accepted after revision: June 22, 2012
Published online: August 7, 2012

Expression of Stanniocalcin 1 as a Potential Biomarker of Gastric Cancer

Takaaki Arigami[a, b] Yoshikazu Uenosono[b] Sumiya Ishigami[a]
Takahiko Hagihara[a] Naoto Haraguchi[a] Daisuke Matsushita[a]
Shigehiro Yanagita[a] Akihiro Nakajo[a] Hiroshi Okumura[a] Shuichi Hokita[c]
Shoji Natsugoe[a, b]

[a]Department of Digestive Surgery, Breast and Thyroid Surgery, Field of Oncology, [b]Molecular Frontier Surgery, Course of Advanced Therapeutics, Graduate School of Medical and Dental Sciences, Kagoshima University, and [c]Department of Surgery, Jiaikai Imamura Hospital, Kagoshima, Japan

Key Words
Blood marker · Gastric cancer · Stanniocalcin 1 · Reverse transcription-polymerase chain reaction · Tumor progression

Abstract
Objective: We investigated stanniocalcin 1 (STC 1) expression to assess its clinical utility as a blood marker in patients with gastric cancer and evaluated its biological impact in terms of tumor aggressiveness. ***Methods:*** Blood specimens from 93 patients with gastric cancer and 21 normal healthy volunteers were assessed by quantitative reverse transcription-polymerase chain reaction for STC 1 mRNA expression. ***Results:*** The relative numbers of STC 1 mRNA copies were significantly higher in gastric cancer cell lines and in blood specimens from patients with gastric cancer than in blood specimens from healthy volunteers ($p = 0.0001$ and $p = 0.003$, respectively). The sensitivity and specificity of STC 1 mRNA expression for discriminating patients with gastric cancer from healthy volunteers were 69.9 and 71.4%, respectively. Furthermore, the sensitivity for STC 1 mRNA was higher than that for serum carcinoembryonic antigen and carbohydrate antigen 19-9. The presence of STC 1 expression was significantly correlated with depth of tumor invasion and tumor stage ($p = 0.032$ and $p = 0.013$, respectively). ***Conclusion:*** Our data strongly suggest that STC 1 is a potentially useful blood marker for predicting biological tumor aggressiveness in patients with gastric cancer.

Copyright © 2012 S. Karger AG, Basel

Introduction

Gastric cancer is one of the most common malignant neoplasms in Japan [1]. In the last decade, the prognosis of patients with unresectable advanced or recurrent gastric cancer has dramatically improved due to the advance of anticancer agents, including novel molecular-targeted drugs such as trastuzumab [2–5]. Furthermore, the 5-year survival rate in patients with resectable advanced gastric cancer has been raised by a combination of curative surgery with D2 lymphadenectomy and adjuvant chemotherapy with S-1 [3]. However, some postoperative patients have a high risk of disease recurrence. Additionally, it is hard to predict patients at increased risk of

KARGER
Fax +41 61 306 12 34
E-Mail karger@karger.ch
www.karger.com

© 2012 S. Karger AG, Basel
0030–2414/12/0833–0158$38.00/0

Accessible online at:
www.karger.com/ocl

Takaaki Arigami, MD, PhD
Department of Digestive Surgery, Field of Oncology, Molecular Frontier Surgery
Course of Advanced Therapeutics, Graduate School of Medical and Dental Sciences
Kagoshima University, 8-35-1 Sakuragaoka, Kagoshima 890-8520 (Japan)
Tel. +81 99 275 5361, E-Mail arigami@m.kufm.kagoshima-u.ac.jp

postoperative disease recurrence. Several investigators have demonstrated the clinical impact of circulating tumor cells (CTC) as an underlying cause of disease recurrence [6–9]. At present, carcinoembryonic antigen (CEA) and carbohydrate antigen 19-9 (CA 19-9) are clinically utilized to monitor CTC as conventional blood markers in patients with gastric cancer. Unfortunately, the sensitivity and specificity of these blood markers are not sufficient to discriminate patients with gastric cancer from healthy controls and to detect subclinical patients with a potential risk of recurrence. Moreover, it is problematic that promising blood markers for patients with gastric cancer are limited in clinical management.

Stanniocalcin (STC) was initially discovered in the corpuscles of Stannius of bony fish; it controls calcium and phosphate homeostasis to prevent hypercalcemia [10–15]. STC 1 is one of the STC family members, and a human cDNA clone encoding the mammalian homolog of STC was first isolated in 1996 [11]. The human STC 1 gene consists of 4 exons, spans 13 kb and is mapped to 8p11.2–p21. Previous studies have demonstrated that STC 1 is involved in various biological mechanisms of tumor progression [16–20]. Furthermore, STC 1 enhances tumor angiogenesis via up-regulation of vascular endothelial growth factor (VEGF) [18]. STC 1 is overexpressed in primary tumor cells of several malignancies, such as carcinomas of the esophagus, stomach, colorectum, breast, lung and ovary [17–19, 21–24]. However, little is understood about the clinical significance of STC 1 expression in blood specimens from patients with gastric cancer.

The purpose of the present study was to investigate STC 1 expression in blood specimens from patients with gastric cancer and to compare the clinical utility of STC 1 with those of conventional serum markers for cancer detection. Additionally, we assessed the relationship between STC 1 expression and clinicopathological features of patients with gastric cancer.

Materials and Methods

Gastric Cancer Cell Lines

Five gastric cancer cell lines (MKN-7, MKN-45, MKN-74, KATO-III and NUGC-4) were cultured in RPMI 1640 (Nissui Pharmaceutical Co., Ltd., Tokyo, Japan) supplemented with 10% fetal calf serum (Mitsubishi Kasei, Tokyo, Japan), 100 U/ml penicillin and 100 U/ml streptomycin. All cancer cell lines were incubated at 37°C in a humidified atmosphere containing 5% CO_2, as described previously [25, 26]. These cell lines were used for reverse transcription-polymerase chain reaction (RT-PCR).

Patients

In the present study, blood specimens were preoperatively collected from 93 patients (64 men and 29 women; age range, 35–87 years; average, 68 years) with gastric cancer who underwent curative gastrectomy with lymphadenectomy at the Kagoshima University Hospital (Kagoshima, Japan) between 2003 and 2005. Patients who received endoscopic treatment, palliative resection, preoperative chemotherapy, and/or radiotherapy were excluded from this study. The study patients were classified and staged on the basis of criteria for the tumor-node-metastasis classification of gastric carcinoma established by the UICC (International Union Against Cancer) [27]. Normal peripheral blood lymphocytes (PBLs) obtained and isolated from 21 healthy volunteers without cancer were used as a control. Moreover, we collected 20 surgical paraffin-embedded archival tissue (PEAT) specimens of resected primary tumor sites from patients enrolled in this study and these PEAT specimens were used for immunohistochemistry (IHC).

All patients provided written, informed consent to specimen collection in accordance with our institutional guidelines.

Enzyme Immunoassay Analysis for the Determination of Serum CEA and CA 19-9

Serum samples were collected for the immunoassay of tumor markers CEA and CA 19-9. Serum concentrations of CEA and CA 19-9 were measured using a commercial enzyme immunoassay kit (Abbott Co., Ltd., Tokyo, Japan). The cutoff values for serum CEA and CA 19-9 levels were 5.0 ng/ml and 37 U/ml, respectively [28].

Blood Processing and RNA Isolation

All blood specimens (5 ml) were preoperatively collected into tubes containing sodium citrate, and blood cells were separated using lymphocyte separation buffer (Gentra Systems, Inc., Minneapolis, Minn., USA). Total RNA was extracted from cell lines and blood specimens using Isogen (Nippon Gene, Toyama, Japan). Total RNA was isolated and purified using phenol-chloroform extraction, as described previously [25, 26]. The concentration and purity of total RNA were examined using a GeneQuant pro UV/Vis spectrophotometer (Amersham Pharmacia Biotech, Cambridge, UK).

Quantitative RT-PCR Analysis

Primer and probe sequences of STC 1 and glyceraldehyde-3-phosphatase dehydrogenase (GAPDH) were designed for quantitative RT-PCR (qRT-PCR) assay. The forward primers, fluorescence resonance energy transfer probe sequence, and reverse primers for STC 1 and GAPDH were as follows: STC 1 (forward), 5′-CACTTCTCCAACAGATACT-3′; (probe), 5′-FAM–CCTGCTGGAATGTGATGAAGACAC–TAMRA-1-3′; (reverse), 5′-CATGTTAGGCCCAATTTTC-3′; GAPDH (forward), 5′-GGGTGTGAACCATGAGAAGT-3′; (probe), 5′-FAM–CAGCAATGCCTCCTGCACCACCAA–TAMRA-1-3′, and (reverse), 5′-GACTGTGGTCATGAGTCCT-3′. The RT-PCR product sizes of STC 1 and GAPDH were 111 and 136 base pair fragments, respectively. The integrity of the RNA was assessed by RT-PCR assay using GAPDH.

All total RNA samples were reverse transcribed using the Advantage RT-for-PCR kit (Clontech Laboratories, Inc., Palo Alto, Calif., USA), as described previously [25, 26]. Samples were

analyzed by qRT-PCR assay using the LightCycler System (Roche Diagnostics, Mannheim, Germany). The reaction mixtures contained cDNA transcribed from 250 ng of RNA using each primer, probe, $MgCl_2$ and LightCycler FastStart DNA Master hybridization probes (Roche). The amplification profile comprised precycling at 95°C for 10 min followed by 40 cycles of denaturation at 95°C for 10 s, annealing for 20 s (60°C for STC 1 and 55°C for GAPDH) and extension at 72°C for 10 s. Plasmids for each marker were synthesized using pT7Blue-2 T-Vector (Novagen, Madison, Wisc., USA) according to the manufacturer's instructions. Standard curves for each assay were generated using the threshold cycles of six serial dilutions of plasmid templates (10^6–10^1 copies). The mRNA copy number was calculated using LightCycler software (Roche). Each assay was repeated in duplicate with positive (cancer cell line), negative (H_2O) and reagent (without cDNA) controls to confirm the validity of the qRT-PCR assay. Absolute copy numbers in qRT-PCR assay were determined on the basis of standard curves with six serial dilutions of plasmid templates. STC 1 mRNA copy numbers were normalized by GAPDH mRNA copy numbers (relative STC 1 mRNA copies; absolute STC 1 mRNA copies/absolute GAPDH mRNA copies).

IHC Analysis

The PEAT sections (3 μm thick) were incubated on slides at 50°C overnight, deparaffinized with xylene and then rehydrated with a graded series of ethanol. These sections were autoclaved in citrate buffer (0.01 mol/l, pH 6.0) at 120°C for 10 min to activate the antigen. Endogenous peroxidase was blocked using peroxidase blocking reagent (DakoCytomation, Carpinteria, Calif., USA) for 10 min after cooling at room temperature. Non-specific binding was blocked at room temperature for 30 min with a serum-free protein block (DakoCytomation). The sections were incubated at 4°C overnight with an anti-human STC 1 polyclonal antibody (Santa Cruz Biotechnology, Inc., Santa Cruz, Calif., USA) diluted 1:50 in Dako antibody diluent with background-reducing components (DakoCytomation). After washing in phosphate-buffered saline (PBS), the reaction for anti-human STC 1 polyclonal antibody was developed by the ABC method (Vectastain ABC kit; Vector Laboratories, Burlingame, Calif., USA) and visualized using diaminobenzidine tetrahydrochloride (DakoCytomation) [29]. PBS without primary antibody was used as a negative control under the same conditions.

Statistical Analysis

Differences in STC 1 mRNA expression between cancer cell lines and normal PBLs from healthy volunteers, and between PBLs from patients with gastric cancer and healthy volunteers, were assessed by the Wilcoxon rank sum test. Receiver operating characteristic (ROC) curves and the area under the curve (AUC) were used to evaluate the predictive ability of STC 1 mRNA expression for discriminating patients with gastric cancer from normal healthy volunteers. The relationship between STC 1 mRNA expression and categorical clinicopathological factors was statistically analyzed by χ^2 and Fisher's exact tests. All statistical calculations were carried out using SAS statistical software (SAS Institute Inc., Cary, N.C., USA). A value of $p < 0.05$ was considered statistically significant.

Table 1. Expression of blood markers in 93 patients with gastric cancer

Blood markers	Expression, n (%)	
	negative	positive
Serum CEA	68 (73.1)	25 (26.9)
Serum CA 19-9	70 (75.3)	23 (24.7)
STC 1	28 (30.1)	65 (69.9)

Results

RT-PCR Analysis of STC 1 mRNA Expression in Cell Lines and Clinical Blood Specimens

We initially assessed STC 1 mRNA expression in five gastric cancer cell lines and clinical blood specimens from 93 patients with gastric cancer and 21 healthy volunteers using qRT-PCR assay.

The relative numbers of STC 1 mRNA copies ranged from 3.15×10^{-5} to 2.97×10^{-3} in gastric cancer cell lines, from 0 to 8.39×10^{-4} in blood specimens of patients with gastric cancer, and from 0 to 2.14×10^{-6} in blood specimens of healthy volunteers. The mean relative numbers of STC 1 mRNA copies (±SD) were $8.47 \times 10^{-4} \pm 1.25 \times 10^{-3}$ in gastric cancer cell lines, $1.02 \times 10^{-5} \pm 8.69 \times 10^{-5}$ in blood specimens of patients with gastric cancer, and $3.44 \times 10^{-7} \pm 6.12 \times 10^{-7}$ in blood specimens of healthy volunteers (fig. 1). Finally, the relative numbers of STC 1 mRNA copies were significantly higher in gastric cancer cell lines and blood specimens of patients with gastric cancer than in blood specimens of healthy volunteers ($p = 0.0001$ and $p = 0.003$, respectively).

Comparison of the Clinical Utility between STC 1 and Conventional Serum Markers for Cancer Detection

ROC analysis statistically demonstrated that the AUC value for cancer detection based on the levels of STC 1 mRNA expression was 0.702 (fig. 2). The values of sensitivity and specificity of STC 1 mRNA were 0.699 and 0.714, respectively. Consequently, RT-PCR analysis demonstrated that 65 of 93 (69.9%) patients were positive for STC 1. On the other hand, positive rates of serum CEA and CA 19-9 in the same population were 26.9 (25/93) and 24.7% (23/93), respectively. Thus, the positive rate of STC 1 mRNA was higher than those of serum CEA and CA 19-9 (table 1).

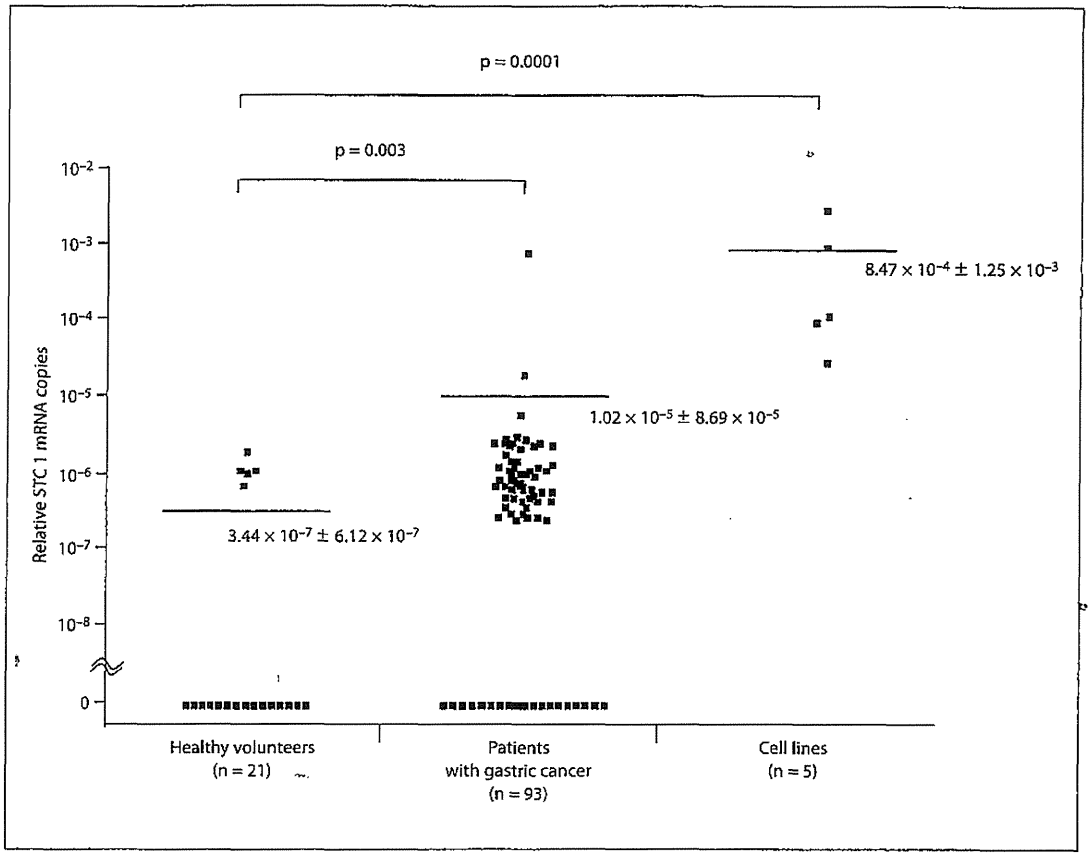

Fig. 1. RT-PCR analysis of STC 1 mRNA expression in cell lines and clinical blood specimens. Horizontal bars indicate mean number of STC 1 mRNA copies.

Correlation between STC 1 Expression and Clinicopathological Findings

To assess the relationship between the status of STC 1 expression and clinicopathological findings, all patients enrolled in this study were divided into two groups based on the presence or absence of STC 1 mRNA expression (positive, n = 65; negative, n = 28).

The status of STC 1 expression was significantly correlated with depth of tumor invasion and stage ($p = 0.032$ and $p = 0.013$, respectively; table 2).

IHC Analysis of STC 1 Protein Expression in Primary Tumor Specimens

To assess STC 1 expression in primary tumor cells, 20 surgical PEAT primary specimens obtained from patients with STC 1-positive expression in blood specimens were used for IHC analysis.

IHC analysis demonstrated STC 1 protein expression in the cytoplasm of tumor cells (fig. 3). Although immunoreactivity for STC 1 was variable in primary tumor cells, STC 1was expressed in all PEAT specimens (fig. 3).

Discussion

In the present study, we examined STC 1 mRNA expression by qRT-PCR assay in blood specimens from patients with gastric cancer and normal healthy volunteers. To assess the clinical utility of STC 1 as a diagnostic biomarker, we next compared the sensitivity of STC 1 with those of conventional serum markers, such as CEA and CA 19-9. Furthermore, we investigated the clinical impact of STC 1 expression in patients with gastric cancer. To our knowledge, this study is the first to demonstrate

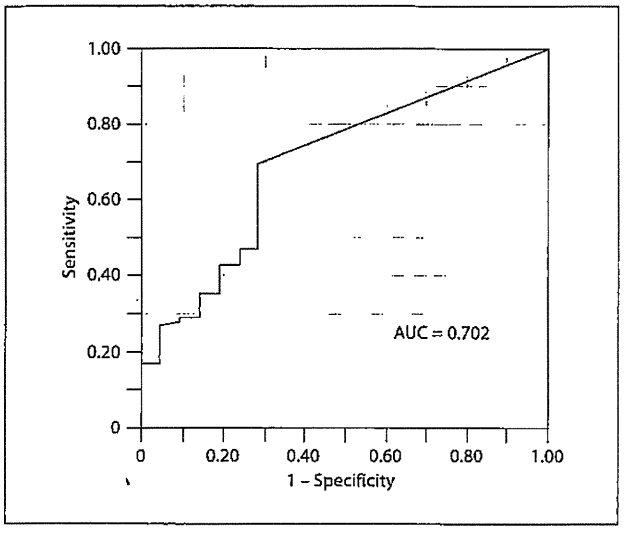

Fig. 2. ROC curve for discriminating patients with gastric cancer from healthy volunteers on the basis of STC 1 mRNA expression. AUC = 0.702.

STC 1 expression in blood specimens from patients with gastric cancer.

Initially, we verified a high level of STC 1 mRNA expression in all gastric cancer cell lines. We next demonstrated high STC 1 expression in blood specimens from patients with gastric cancer, in comparison with those from normal healthy volunteers. Moreover, the sensitivity of STC 1 mRNA was higher than those of serum CEA and CA 19-9 in terms of diagnostic efficacy. Similarly, Du et al. [24] reported that the level of STC 1 mRNA in blood specimens from patients with non-small cell lung cancer was significantly higher than in blood specimens from patients with benign pulmonary disease. Consequently, they concluded that STC 1 is a potential biomarker for patients with non-small cell lung cancer [24]. These results suggest that STC 1 is one of the candidate blood markers for monitoring CTC in patients with selected cancers, including gastric cancer. Currently, chemotherapy is widely performed in patients with unresectable advanced or recurrent gastric cancer. However, it is difficult to assess its effect precisely using conventional examinations such as a blood test for serum CEA and CA 19-9, gastrointestinal fiberscopy, double-contrast gastrography and computed tomography. Matsusaka et al. [30] reported that the monitoring assay of CTC is a useful tool for the assessment of the response to chemotherapy in patients with advanced gastric cancer. Further studies will be needed to verify the clinical efficacy of the STC 1-targeting qRT-PCR assay for predicting chemotherapeutic effects in patients with unresectable advanced or recurrent gastric cancer.

In the present study, we demonstrated that the presence of STC 1 expression was significantly correlated with tumor aggressiveness, such as depth of tumor invasion and stage. The 5-year survival rates of our patients with STC 1-positive and -negative expression were 64.4 and

Table 2. Correlation between STC 1 expression and clinicopathological findings in patients with gastric cancer

Factors	STC 1 expression, n (%)		p value
	negative (n = 28)	positive (n = 65)	
Gender			
Male	21 (75.0)	43 (66.1)	0.470
Female	7 (25.0)	22 (33.9)	
Age			
<70 years	13 (46.4)	32 (49.2)	0.825
>70 years	15 (53.6)	33 (50.8)	
Tumor location			
Upper	10 (35.7)	21 (32.3)	0.925
Middle	8 (28.6)	21 (32.3)	
Lower	10 (35.7)	23 (35.4)	
Histological type			
Differentiated	15 (53.6)	31 (47.7)	0.656
Undifferentiated	13 (46.4)	34 (52.3)	
Tumor size			
<50 mm	12 (42.9)	21 (32.3)	0.353
>50 mm	16 (57.1)	44 (67.7)	
Depth of tumor invasion			
pT_1–T_2	14 (50.0)	17 (26.1)	0.032
pT_3-T_4	14 (50.0)	48 (73.9)	
Lymph node metastasis			
Negative	15 (53.6)	22 (33.9)	0.106
Positive	13 (46.4)	43 (66.1)	
Stage			
I	14 (50.0)	14 (21.5)	0.013
II–IV	14 (50.0)	51 (78.5)	
Lymphatic invasion			
Negative	13 (46.4)	17 (26.1)	0.089
Positive	15 (53.6)	48 (73.9)	
Venous invasion			
Negative	13 (46.4)	18 (27.7)	0.096
Positive	15 (53.6)	47 (72.3)	

Except for tumor location (χ^2 test), p values were examined by Fisher's exact test. pT_1 = Invasion of lamina propria or submucosa; pT_2 = invasion of muscularis propria; pT_3 = invasion of subserosa; pT_4 = penetration of serosa without invasion of adjacent structures or invasion of adjacent structures.

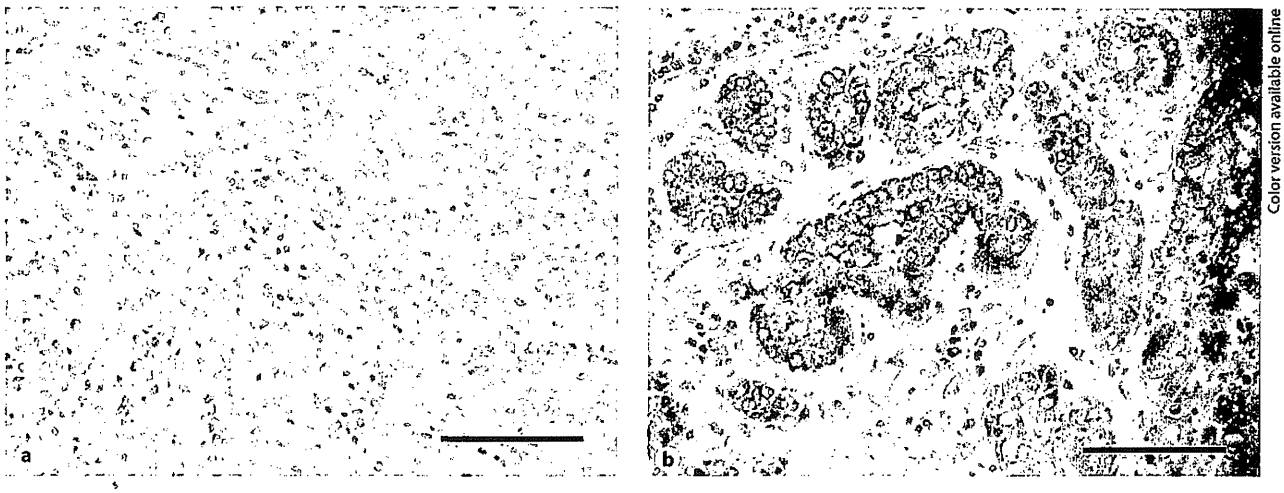

Fig. 3. Representative IHC of STC 1 protein expression in primary gastric tumor specimens. **a** Tumor cells with weak expression of STC 1. **b** Tumor cells with strong expression of STC 1. Scale bars = 100 μm (original magnification ×400).

79.4%, respectively. However, none of these differences reached statistical significance (data not shown). There are some possible explanations for this result: (a) The follow-up period was short (median, 25 months); (b) Patients receiving postoperative chemotherapy were included in this study and the selection criteria for postoperative chemotherapy were ambiguous in terms of the historical background. (c) The sample size may be too small for the identification of valid differences. Although further large studies are required to validate our results, the assessment of STC 1 expression in peripheral blood specimens might allow the preoperative prediction of aggressive disease behavior that has substantial influence on the therapeutic management of patients with gastric cancer.

To date, the biological role of STC 1 expression in tumor cells has not been sufficiently elucidated. However, Liu et al. [17] reported that the anti-apoptotic effect of STC 1 was inhibited by neutralizing anti-STC 1 monoclonal antibodies in in vitro assays. Furthermore, He et al. [18] reported that STC 1 promoted expression of VEGF related to angiogenesis via the activation of PKCβ II and ERK 1/2 pathways in in vitro assays. In this study, we confirmed STC 1 expression in blood specimens from patients with gastric cancer. Therefore, in the near future, it is necessary to elucidate the detailed mechanism of the STC 1 signaling pathway in gastric cancer.

In conclusion, we demonstrated that STC 1 is expressed in CTC and that its expression is closely correlated with tumor progression. Further studies on its biological role might lead to a novel molecular therapy that suppresses the STC 1 signaling pathway in patients with gastric cancer.

Acknowledgment

We thank Ms. A. Harada for technical assistance. This work was supported in part by a grant-in-aid (No. 22791256) for scientific research from the Ministry of Education, Science, Sports, and Culture of Japan.

Disclosure Statement

The authors have no conflicts of interest.

References

1 Statistics and Information Department, Ministry of Health, Labor, and Welfare: Vital Statistics of Japan 2004. Tokyo, Health and Welfare Statistics Association, 2006.
2 Ohtsu A: Current status and future prospects of chemotherapy for metastatic gastric cancer: a review. Gastric Cancer 2005;8:95–102.
3 Sakuramoto S, Sasako M, Yamaguchi T, Kinoshita T, Fujii M, Nashimoto A, Furukawa H, Nakajima T, Ohashi Y, Imamura H, Higashino M, Yamamura Y, Kurita A, Arai K, ACTS-GC Group: Adjuvant chemotherapy for gastric cancer with S-1, an oral fluoropyrimidine. N Engl J Med 2007;357:1810–1820.

4 Koizumi W, Narahara H, Hara T, Takagane A, Akiya T, Takagi M, Miyashita K, Nishizaki T, Kobayashi O, Takiyama W, Toh Y, Nagaie T, Takagi S, Yamamura Y, Yanaoka K, Orita H, Takeuchi M: S-1 plus cisplatin versus S-1 alone for first-line treatment of advanced gastric cancer (SPIRITS trial): a phase III trial. Lancet Oncol 2008;9:215–221.
5 Bang YJ, Van Cutsem E, Feyereislova A, Chung HC, Shen L, Sawaki A, Lordick F, Ohtsu A, Omuro Y, Satoh T, Aprile G, Kulikov E, Hill J, Lehle M, Rüschoff J, Kang YK, ToGA Trial Investigators: Trastuzumab in combination with chemotherapy versus chemotherapy alone for treatment of HER2-positive advanced gastric or gastro-oesophageal junction cancer (ToGA): a phase 3, open-label, randomised controlled trial. Lancet 2010;376:687–697.
6 Cristofanilli M, Budd GT, Ellis MJ, Stopeck A, Matera J, Miller MC, Reuben JM, Doyle GV, Allard WJ, Terstappen LW, Hayes DF: Circulating tumor cells, disease progression, and survival in metastatic breast cancer. N Engl J Med 2004;351:781–791.
7 Cohen SJ, Punt CJ, Iannotti N, Saidman BH, Sabbath KD, Gabrail NY, Picus J, Morse M, Mitchell E, Miller MC, Doyle GV, Tissing H, Terstappen LW, Meropol NJ: Relationship of circulating tumor cells to tumor response, progression-free survival, and overall survival in patients with metastatic colorectal cancer. J Clin Oncol 2008;26:3213–3221.
8 Hiraiwa K, Takeuchi H, Hasegawa H, Saikawa Y, Suda K, Ando T, Kumagai K, Irino T, Yoshikawa T, Matsuda S, Kitajima M, Kitagawa Y: Clinical significance of circulating tumor cells in blood from patients with gastrointestinal cancers. Ann Surg Oncol 2008;15:3092–3100.
9 Krebs MG, Sloane R, Priest L, Lancashire L, Hou JM, Greystoke A, Ward TH, Ferraldeschi R, Hughes A, Clack G, Ranson M, Dive C, Blackhall FH: Evaluation and prognostic significance of circulating tumor cells in patients with non-small-cell lung cancer. J Clin Oncol 2011;29:1556–1563.
10 Chang AC, Janosi J, Hulsbeek M, de Jong D, Jeffrey KJ, Noble JR, Reddel RR: A novel human cDNA highly homologous to the fish hormone stanniocalcin. Mol Cell Endocrinol 1995;112:241–247.
11 Olsen HS, Cepeda MA, Zhang QQ, Rosen CA, Vozzolo BL: Human stanniocalcin: a possible hormonal regulator of mineral metabolism. Proc Natl Acad Sci USA 1996;93:1792–1796.
12 Wagner GF, Jaworski EM, Haddad M: Stanniocalcin in the seawater salmon: structure, function, and regulation. Am J Physiol 1998;274:1177–1185.
13 Chang AC, Reddel RR: Identification of a second stanniocalcin cDNA in mouse and human: stanniocalcin 2. Mol Cell Endocrinol 1998;141:95–99.
14 Ishibashi K, Imai M: Prospect of a stanniocalcin endocrine/paracrine system in mammals. Am J Physiol Renal Physiol 2002;282:367–375.
15 Chang AC, Jellinek DA, Reddel RR: Mammalian stanniocalcins and cancer. Endocr Relat Cancer 2003;10:359–373.
16 Yeung HY, Lai KP, Chan HY, Mak NK, Wagner GF, Wong CK: Hypoxia-inducible factor-1-mediated activation of stanniocalcin-1 in human cancer cells. Endocrinology 2005;146:4951–4960.
17 Liu G, Yang G, Chang B, Mercado-Uribe I, Huang M, Zheng J, Bast RC, Lin SH, Liu J: Stanniocalcin 1 and ovarian tumorigenesis. J Natl Cancer Inst 2010;102:812–827.
18 He LF, Wang TT, Gao QY, Zhao GF, Huang YH, Yu LK, Hou YY: Stanniocalcin-1 promotes tumor angiogenesis through up-regulation of VEGF in gastric cancer cells. J Biomed Sci 2011;18:39.
19 Shirakawa M, Fujiwara Y, Sugita Y, Moon JH, Takiguchi S, Nakajima K, Miyata H, Yamasaki M, Mori M, Doki Y: Assessment of stanniocalcin-1 as a prognostic marker in human esophageal squamous cell carcinoma. Oncol Rep 2012;27:940–946.
20 Yeung BH, Law AY, Wong CK: Evolution and roles of stanniocalcin. Mol Cell Endocrinol 2012;349:272–280.
21 Wascher RA, Huynh KT, Giuliano AE, Hansen NM, Singer FR, Elashoff D, Hoon DS: Stanniocalcin-1: a novel molecular blood and bone marrow marker for human breast cancer. Clin Cancer Res 2003;9:1427–1435.
22 Nakagawa T, Martinez SR, Goto Y, Koyanagi K, Kitago M, Shingai T, Elashoff DA, Ye X, Singer FR, Giuliano AE, Hoon DS: Detection of circulating tumor cells in early-stage breast cancer metastasis to axillary lymph nodes. Clin Cancer Res 2007;13:4105–4110.
23 Tamura S, Oshima T, Yoshihara K, Kanazawa A, Yamada T, Inagaki D, Sato T, Yamamoto N, Shiozawa M, Morinaga S, Akaike M, Kunisaki C, Tanaka K, Masuda M, Imada T: Clinical significance of STC1 gene expression in patients with colorectal cancer. Anticancer Res 2011;31:325–329.
24 Du YZ, Gu XH, Li L, Gao F: The diagnostic value of circulating stanniocalcin-1 mRNA in non-small cell lung cancer. J Surg Oncol 2011;104:836–840.
25 Arigami T, Natsugoe S, Uenosono Y, Arima H, Mataki Y, Ehi K, Yanagida S, Ishigami S, Hokita S, Aikou T: Lymphatic invasion using D2–40 monoclonal antibody and its relationship to lymph node micrometastasis in pN0 gastric cancer. Br J Cancer 2005;93:688–693.
26 Arigami T, Natsugoe S, Uenosono Y, Mataki Y, Ehi K, Higashi H, Arima H, Yanagida S, Ishigami S, Hokita S, Aikou T: Evaluation of sentinel node concept in gastric cancer based on lymph node micrometastasis determined by reverse transcription-polymerase chain reaction. Ann Surg 2006;243:341–347.
27 Edge SB, Byrd DR, Compton CC, Fritz AG, Greene FL, Trotti A (eds): AJCC Cancer Staging Manual, ed 7. New York, Springer, 2010.
28 Oue N, Sentani K, Noguchi T, Ohara S, Sakamoto N, Hayashi T, Anami K, Motoshita J, Ito M, Tanaka S, Yoshida K, Yasui W: Serum olfactomedin 4 (GW112, hGC-1) in combination with Reg IV is a highly sensitive biomarker for gastric cancer patients. Int J Cancer 2009;125:2383–2392.
29 Hsu SM, Raine L, Fanger H: Use of avidin-biotin-peroxidase complex (ABC) in immunoperoxidase techniques: a comparison between ABC and unlabeled antibody (PAP) procedures. J Histochem Cytochem 1981;29:577–580.
30 Matsusaka S, Chin K, Ogura M, Suenaga M, Shinozaki E, Mishima Y, Terui Y, Mizunuma N, Hatake K: Circulating tumor cells as a surrogate marker for determining response to chemotherapy in patients with advanced gastric cancer. Cancer Sci 2010;101:1067–1071.

Development 139, 667-677 (2012) doi:10.1242/dev.072272
© 2012. Published by The Company of Biologists Ltd

Genetic ablation of *Rest* leads to in vitro-specific derepression of neuronal genes during neurogenesis

Hitomi Aoki[1], Akira Hara[2], Takumi Era[3], Takahiro Kunisada[1] and Yasuhiro Yamada[4,5,*]

SUMMARY

Rest (RE1-silencing transcription factor, also called Nrsf) is involved in the maintenance of the undifferentiated state of neuronal stem/progenitor cells in vitro by preventing precocious expression of neuronal genes. However, the function of *Rest* during neurogenesis in vivo remains to be elucidated because of the early embryonic lethal phenotype of conventional *Rest* knockout mice. In the present study, we have generated *Rest* conditional knockout mice, which allow the effect of genetic ablation of *Rest* during embryonic neurogenesis to be examined in vivo. We show that *Rest* plays a role in suppressing the expression of neuronal genes in cultured neuronal cells in vitro, as well as in non-neuronal cells outside of the central nervous system, but that it is dispensable for embryonic neurogenesis in vivo. Our findings highlight the significance of extrinsic signals for the proper intrinsic regulation of neuronal gene expression levels in the specification of cell fate during embryonic neurogenesis in vivo.

KEY WORDS: Rest (Nrsf), Mouse model, Neurogenesis

INTRODUCTION

The establishment and maintenance of neuronal identity underlie the core of neuronal development. The transcriptional repressor RE1-silencing transcription factor [Rest; also known as neuron-restrictive silencer factor (Nrsf)], was initially discovered as a negative regulator of neuron-specific genes in non-neuronal cells (Chong et al., 1995; Schoenherr and Anderson, 1995). Rest is expressed throughout early development, where it represses the expression of neuronal genes and is involved in the transcriptional silencing of neuronal promoters in conjunction with CoRest (Rcor1/2) (Ballas et al., 2001), which recruits additional silencing machinery, including the methyl DNA-binding protein MeCP2, histone deacetylase (HDAC) and the histone H3K9 methyltransferase G9a (Ehmt2) (Andres et al., 1999; Lunyak et al., 2002; Roopra et al., 2004; Shi et al., 2003; You et al., 2001). Rest targets include a number of genes encoding ion channels, neurotrophins, synaptic vesicle proteins and neurotransmitter receptors (Bruce et al., 2004; Johnson et al., 2006; Otto et al., 2007). Indeed, a targeted mutation of *Rest* in mice caused derepression of neuron-specific tubulin in a subset of non-neuronal tissues, leading to embryonic lethality (Chen et al., 1998).

Mosaic inhibition of *Rest* in chicken embryos using a dominant-negative form of *Rest* also caused derepression of neuronal tubulin, as well as several other neuronal target genes, not only in non-neuronal tissues but also neuronal progenitors (Chen et al., 1998). These results suggest that *Rest* is required to repress the expression of neuronal genes in undifferentiated neuronal tissue. Expression of Rest is highest in embryonic stem cells (ESCs) and is downregulated as ESCs differentiate into neuronal stem cells (NSCs), and it is completely silenced in mature adult neuronal cells (Ballas et al., 2005). Given the fact that Rest represses the expression of a large number of neuronal genes, it is reasonable to expect that it plays a central role in the inhibition of the precocious expression of neuronal genes in NSCs, and that its downregulation upon receipt of neuronal differentiation cues permits the robust expression of differentiation-related neuronal genes, resulting in terminal differentiation (Ballas et al., 2005).

In addition to the involvement of Rest in neurogenesis, recent studies have demonstrated that Rest modulates glial lineage elaboration (Abrajano et al., 2009; Kohyama et al., 2010), suggesting that it also mediates the coupling of neurogenesis and gliogenesis, which might contribute to the neuronal-glial interactions that are associated with synaptic and neuronal network plasticity and homeostasis in the brain. Despite the expectation of a fundamental role of Rest in brain development, the function of Rest in NSCs and neuronal progenitors in the brain in vivo remains to be elucidated. *Rest* null mice survive to embryonic day (E) 9 without obvious morphological defects, by which time all three germ layers and the neural tube have formed, clearly demonstrating that neuronal progenitors can develop in vivo in the absence of *Rest* (Chen et al., 1998). However, *Rest* null mice die by E11.5 accompanied by gross morphological changes starting ~E9.5. This early embryonic lethality has precluded further analysis of the role of *Rest* in the maintenance and differentiation of NSCs and neural progenitor cells (NPCs) in vivo.

In addition to the possible role of *Rest* in neuronal/glial development, recent studies have indicated that the breakdown of these processes accompanies and promotes neurodegenerative disorders. The disruption of the interaction of Rest with its target genes was reported in epileptic seizures (Bassuk et al., 2008), Huntington's disease (Zuccato et al., 2007) and Down's syndrome (Canzonetta et al., 2008; Lepagnol-Bestel et al., 2009). In these disorders, Rest dysfunction is suggested to be a cause of aberrant changes in neuronal gene expression. Considering that abnormal expression of Rest has been seen in a variety of neurological and neurodegenerative diseases, it is important to uncover the

[1]Department of Tissue and Organ Development and [2]Department of Tumor Pathology, Regeneration, and Advanced Medical Science, Gifu University Graduate School of Medicine, Gifu, 501-1194, Japan. [3]Division of Molecular Neurobiology, Institute of Molecular Embryology and Genetics, Kumamoto University, Kumamoto 860-0811, Japan. [4]PRESTO, Japan Science and Technology Agency, 4-1-8 Honcho Kawaguchi, Saitama, Japan. [5]Center for iPS Cell Research and Application (CiRA), Institute for Integrated Cell-Material Sciences (iCeMS), Kyoto University, Kyoto 606-8507, Japan.

*Author for correspondence (y-yamada@cira.kyoto-u.ac.jp)

Accepted 18 December 2011